ISPRS Journal of Photogrammetry and Remote Sensing 234 (2026) 337–354

Contents lists available at ScienceDirect

ISPRS Journal of Photogrammetry and Remote Sensing

journal homepage: www.elsevier.com/locate/isprsjprs

Towards operational tracking of weekly crop progress using VIIRS land surface phenology product across the continental United States

Naeem Abbas Malik [a,b], Xiaoyang Zhang [a,*], Yu Shen [a], Zhengwei Yang [c], Yongchang Ye [a], Yuxia Liu [a]

[a] Geospatial Sciences Center of Excellence, Department of Geography and Geospatial Sciences, South Dakota State University, Brookings, SD 57007, USA
[b] Institute of Geoinformation and Earth Observation, Pir Mehr Ali Shah Arid Agriculture University Rawalpindi, Murree Road, Rawalpindi 46300, Pakistan
[c] Research and Development Division, National Agricultural Statistics Services, United States Department of Agriculture, Washington, DC 20250, USA

ARTICLE INFO

Keywords:
Land surface phenology
Visible Infrared Imaging Radiometer Suite (VIIRS)
Crop phenology
Crop progress
Crop growth

ABSTRACT

Monitoring crop progress is crucial for optimizing agricultural productivity, assessing crop health, predicting yields, assessing food security, and mitigating climate change risks. Field surveys and expert assessments, such as crop progress reports (CPR) by National Agricultural Statistics Service (NASS) of United States Department of Agriculture (USDA), lack spatial details and may contain temporal gaps. However, temporally and spatially detailed crop phenological progress is needed for enhancing the decision-making process and for improving crop management practices. Although crop progress derived from satellite data does not inherently align with the cumulative crop progress reported in NASS-CPR, it provides continuous observations of spatial and temporal crop growth. The long-term VIIRS (Visible Infrared Imaging Radiometer Suite) global land surface phenology (GLSP) product (VNP22Q2) from NASA (National Aeronautics and Space Administration) provides valuable assets for assessing its alignments and discrepancies with NASS-CPR at state levels, offering spatially explicit patterns of crop progress. This study was to investigate and evaluate the capability of VIIRS-GLSP for tracking weekly NASS crop progress of five major crops (corn, soybean, cotton, rice and spring wheat) across the Continental United States (CONUS). We developed exponential models of crop growth times in day of the year (DOY) to bridge VIIRS-GLSP cumulative distribution function (CDF) and NASS-CPR for each crop type and phenological stage at a state level from 2013 to 2021 to produce NASS-CPR like GLSP crop progress. The models were then evaluated by predicting crop progress in the year 2022 using calibrated VIIRS-GLSP data. Finally, we adjusted the GLSP crop progress predictions at a pixel level to produce weekly crop progress equivalent to NASS-CPR. The results revealed the capability of VIIRS-GLSP product for monitoring crop progress. The inter-annual variations among VIIRS-GLSP phenometrics and the corresponding NASS-CPR crop growth stages were coincident. The GLSP crop progress derived from calibrated VIIRS-GLSP phenometrics was able to track the NASS-CPR at a state level with varied temporal differences across the crop stages. The GLSP crop progress presented relatively small Root Mean Square Error (RMSE) values (< 5 days) for the growth stages of soybean blooming, setting pods and dropping leaves stages. Similarly, the GLSP crop progress estimated corn silking progress with a RMSE less than 6 days in most states. For cotton, rice, and spring wheat, the GLSP crop progress showed strong performance across most stages and states. Further, bias adjustment based on weekly NASS-CPR percentages effectively improved the pixel distributions of the given weekly GLSP crop progress, which produced crop progress consistent with field-based NASS CPR observations while preserving the logical sequence of crop development. The proposed framework provides a robust and scalable method for generating spatially explicit and temporally consistent crop progress estimates for operational crop monitoring.

1. Introduction

Crop phenology is a fundamental aspect of agricultural science, as it characterizes the time of recurring plant growth and development phases. Monitoring crop phenology is crucial for assessing crop health and guiding efficient application of fertilizers, irrigation, herbicides, and

* Corresponding author.
E-mail address: xiaoyang.zhang@sdstate.edu (X. Zhang).

https://doi.org/10.1016/j.isprsjprs.2026.02.032
Received 20 May 2025; Received in revised form 8 December 2025; Accepted 26 February 2026
Available online 3 March 2026

pesticides, as well as for managing harvesting operations effectively (Brown et al. 2012; Luo et al. 2020; Walthall et al. 2013). Furthermore, crop phenology serves as valuable information for researchers and policy makers in optimizing agricultural productivity, predicting yields, assessing food security, and mitigating extreme weather risks to agricultural systems (Chen et al. 2018; Franch et al. 2015). Analyzing long-term trends in crop phenology provides valuable insights into the adaptation and resilience of cropping ecosystems under changing weather conditions, contributing to sustainable agricultural practices and food security.

Crop phenology is usually determined by ground observations of key crop growth stages, photographs from unmanned aerial vehicles (UAVs) or cameras mounted on towers (PhenoCam), and satellite imagery. Field surveys and expert assessments have played a critical role in crop monitoring for decades, such as crop progress reports (CPR) released by National Agricultural Statistics Service (NASS) of United States Department of Agriculture (USDA). NASS-CPR reports weekly percentage of a given crop type that has reached a specific growth stage at a state or Agricultural Statistics District (ASD) level following NASS standard definitions (NASS 2018), but it is laborious, time consuming, and subjective in nature (Sakamoto et al. 2010; Shen et al. 2022). However, it is unable to offer spatial details of crop phenological stages at the reporting date and may contain temporal gaps due to no/low-quality reports and restricted fieldworks (Gao et al. 2017; Seo et al. 2019). Temporally and spatially detailed crop phenological progress is needed for enhancing the decision-making process and for improving crop management practices (Gao et al. 2017).

Satellite images or UAVs retrieve crop phenology using time series vegetation indices that characterize the crop dynamics in canopy structure or greenness (Thapa et al. 2021; Zhang et al. 2018a). Although using UAV images can largely avoid temporal gaps that commonly induce crop phenology retrieval uncertainties, they can only observe limited crop species and geographical coverages. For decades, crop phenology has been extensively estimated from local to global scales using satellite observations including the Advanced Very High-Resolution Radiometer (AVHRR) (Gim et al. 2020; Sehgal et al. 2011; Wu et al. 2021; Zhang et al. 2017a), the Moderate Resolution Imaging Spectrometer (MODIS) (Li et al. 2014; Onojeghuo et al. 2018; Sakamoto et al. 2005), the Visible Infrared Imaging Radiometer Suite (VIIRS) (Liu et al. 2018; Zhang et al. 2018b), and the Landsat-series and Sentinel-2 datasets (Kosczor et al. 2022; Sisheber et al. 2022; Tran et al. 2023). Although field and satellite-based crop phenology observations show some degrees of consistency in phenological stages (Diao 2020; Gao et al. 2017; Gao and Zhang 2021), differences in their physical definitions (Fig. 1) along with spatial and temporal inconsistencies make it challenging to directly derive crop progress from satellite-based crop phenology detections. Various approaches have been proposed to address these challenges. Sakamoto et al. (2011) applied a shape-model algorithm to estimate corn progress using MODIS data and field observations. The estimated corn progress was comparable to NASS-CPR at an ASD level across Illinois and Iowa. Gao et al. (2017) proposed an algorithm to fuse Landsat-MODIS time series to further enhance the spatial details of corn and soybean progress in Iowa. Diao (2020) demonstrated that crop progress derived from a combination of different crop phenology detection algorithms aligned better with field-observations. Zhang et al. (2020) proposed a Spatiotemporal Shape Mode Matching (SSMM) algorithm to fuse Harmonized Landsat and Sentinel-2 (HLS) and VIIRS time series for enhancing field-scale vegetation phenology detections, which was further utilized for post-season and near real-time crop progress mapping across the mid-western Corn Belt region (Shen et al. 2022; Shen et al. 2023). Liu et al. (2018) proposed an algorithm to detect crop progress in near real-time using historical MODIS and timely available VIIRS data, which demonstrated high-correlations between 500-m VIIRS phenometrics and NASS-CPR data. Collectively, these efforts made significant contributions to crop progress monitoring by (1) improving the spatial details of crop progress from 500-m to 30-m; (2) providing early frameworks for linking satellite-derived land surface phenology to physiological crop growth stages; (3) decreasing the inherent temporal shifts between NASS-CPR and remotely sensed crop progress; and (4) revolutionizing the timeliness of crop progress monitoring from post-season to near real-time. Despite these advances, none of the existing approaches established a systematic and scalable framework for linking operational land surface phenology products to the cumulative weekly crop progress percentages reported by NASS-CPR and further predicted pixel-based crop growth stages characterized in NASS-CPR. Fully proxying NASS-CPR using remotely sensed crop

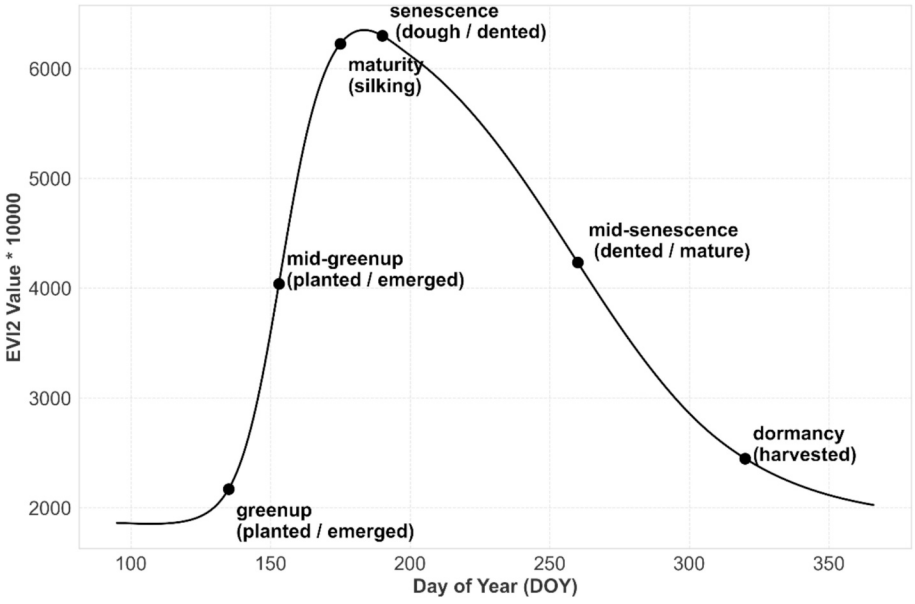

Fig. 1. EVI2 seasonal trajectory for a representative corn pixel illustrating relationship of key land surface phenology transition dates (greenup onset, mid-greenup phase, maturity onset, senescence onset, mid-senescence phase and dormancy onset) with major corn growth stages (planted, emerged, silking, dough, dented, mature and harvested). Although these transitions broadly correspond to physiological corn growth stages, their physical definitions differ from corn growth progress observations in NASS-CPR.

phenology therefore remains challenging over the diverse crop landscapes, various crop species, and different crop phenological stages across the continental United States (CONUS) region.

The VIIRS global land surface phenology (VIIRS-GLSP) product (VNP22Q2) from NASA (National Aeronautics and Space Administration) provides consistent and continuous phenological metrics (phenometrics) since 2013 (Zhang et al. 2024). The VIIRS-GLSP phenometrics (greenup onset, mid-greenup phase, maturity onset, senescence onset, mid-senescence phase and dormancy onset) are crucial for monitoring crop phenology across state, regional and global scales. The long-term VIIRS-GLSP product provides valuable assets for monitoring crop growth with spatially explicit patterns of crop progress that are unavailable in NASS-CPR. However, VIIRS-GLSP pixel-based phenology does not inherently align with the cumulative crop progress reported in NASS-CPR. Bridging VIIRS-derived crop phenology and NASS-CPR field-based crop progress offers a promising opportunity to generate VIIRS-GLSP based spatially distributed weekly crop progress estimates that are equivalent to NASS-CPR product.

This study, therefore, aims to investigate and evaluate the capability of VIIRS-GLSP derived crop phenology to track weekly NASS crop progress data. We established models using VIIRS-GLSP crop phenology for estimating crop progress with spatial distributions at key development stages of five major crops that are corn, soybean, cotton, rice, and spring wheat across the CONUS. The objectives were to: (1) establish the correlations between long-term VIIRS-GLSP and NASS-CPR observations; (2) estimate crop progress using VIIRS-GLSP at the state level in each week of growing season; and (3) predict the pixel-based spatial pattern of crop progress equivalent to state-based NASS-CPR using VIIRS-GLSP.

2. Study area and datasets

2.1. Study area

We focused on the major crop-growing states for five major crops (corn, soybean, cotton, rice, and spring wheat) in the CONUS (Fig. 2). The investigation was performed for corn and soybean in thirteen states, cotton in fifteen states, rice in six states, and spring wheat in six states.

2.2. Data

2.2.1. VIIRS global land surface phenology product

The VIIRS-GLSP product is produced using the Hybrid Piecewise Logistic Model (HPLM) that models temporal trajectory of two-band enhanced vegetation index (EVI2) (Zhang 2015). The HPLM smooths the high-quality VIIRS EVI2 time series using background EVI2 determination, moving average, moving median, and Savitzky-Golay filters. Then, it reconstructs the time series by fitting the temporal curve with logistical models. Finally, the HPLM identifies the phenological transition dates during the growing season using local extreme of curvature change rates that are calculated from the reconstructed EVI2 curve. The product publishes six phenometrics of phenological transition dates that are greenup onset, mid-greenup, maturity onset, senescence onset, mid-senescence, and dormancy onset, which are explained in Table 1 (Zhang et al. 2024). In this study, we downloaded VIIRS-GLSP product data at a spatial resolution of 500-m from NASA's Land Processes Distributed Active Archive Center (LP DAAC) located at the USGS Earth Resources Observation and Science (EROS) center (https://e4ftl01.cr.usgs.gov/VIIRS/) for the years 2013 to 2022 in the corresponding states as highlighted in the study area map (Fig. 2).

2.2.2. NASS cropland data layer

Cropland Data Layer (CDL) provides crop type information at 30 m spatial resolution across the COUNS since 2008 (Boryan et al. 2011). The accuracy of CDL for major crops is reported to be 85–95% particularly in large agricultural states. We downloaded CDL data from the year 2013 to 2022 from USDA NASS (https://nassgeodata.gmu.edu/CropScape), which was used to define pure crop pixels within the VIIRS-GLSP product footprint (500-m).

2.2.3. NASS crop progress reports

NASS compiles crop progress data through weekly surveys conducted by approximately 4,000 trained observers, including farmers, extension agents, and agribusiness professionals. These non-probability

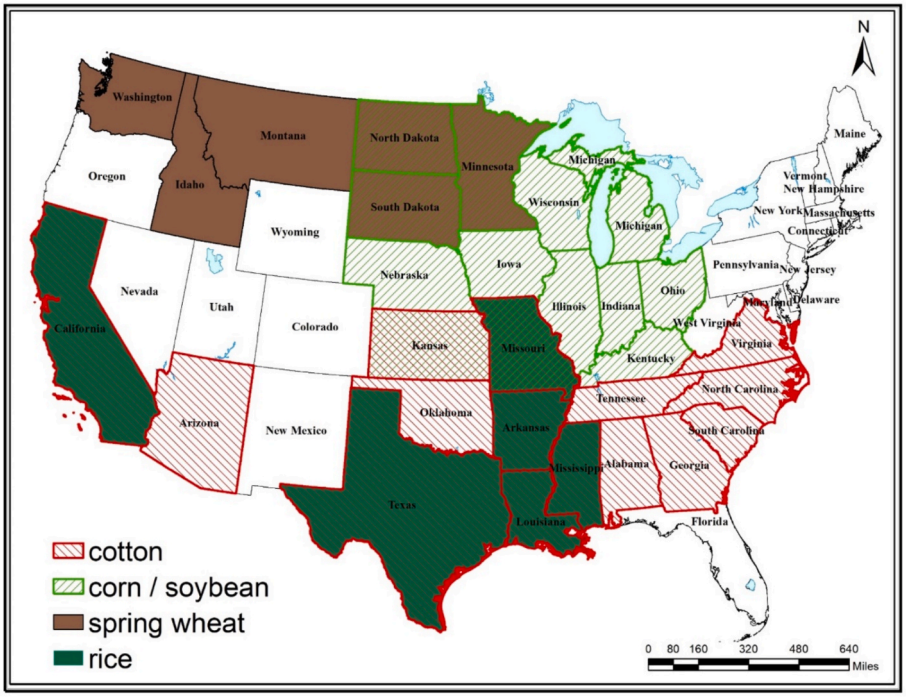

Fig. 2. Study area map with major crop growing states.

Table 1
Details of phenological transition dates provided by VIIRS-GLSP.

Phenology layers	phenological dates	Description
Onset_Greenness_Increase	greenup onset	The date on which greenness starts increasing, greenup onset, start of growing season or start of spring
Onset_Greenness_Maximum	maturity onset	The date within the growing season on which greenness reaches maximum, maturity onset or end of spring
Onset_Greenness_Decrease	senescence onset	The date on which greenness starts decreasing, senescence onset or start of fall
Onset_Greenness_Minimum	dormancy onset	The date within the growing season on which greenness reaches minimum, dormancy onset, end of growing season, or end of fall
Date_Mid_Greenup_Phase	mid-greenup	the date at a mid-greenup phase, mid-greenup phase or middle of spring
Date_Mid_Senescence_Phase	mid-senescence	the date at a mid-senescence phase, mid-senescence phase or middle of fall

surveys provide estimates of the cumulative progress of key growth stages for major crops, expressed as areal percentages at the state level. The crop progress percentages reflect the proportion of acres where at least 50% of plants have reached or surpassed a given phenological stage. The collected data undergo a thorough review for consistency before being aggregated and published in state and national-level reports. These reports, released weekly from April to November, provide insights into crop development and conditions throughout the growing season. The data is publicly available at USDA NASS (https://usda.library.cornell.edu/concern/publications/8336h188j).

3. Analytical methods

The methodology workflow is presented in Fig. 3. First, we calculated the cumulative distributive functions (CDF) for VIIRS-GLSP metrics in each growing stage and each selected crop species (corn, soybean, cotton, rice, and spring wheat) during 2013–2021. Second, we developed exponential models of crop growth times in day of the year (DOY) between VIIRS-GLSP CDF and NASS-CPR for each crop type and phenological stage at a state level. Third, we evaluated models by predicting the crop progress data in the year 2022 using VIIRS-GLSP data. Finally, we adjusted the VIIRS-GLSP predictions at a pixel level to produce crop progress that was equivalent to the weekly crop progress from NASS-CPRs.

3.1. Bridging crop progress derived from VIIRS-GLSP and NASS-CPR

3.1.1. Reconstruction of cumulative distribution functions

A cumulative distribution function (CDF) was generated for each VIIRS-GLSP phenometrics and crop type at a state level. At a given state and crop type, the pure 500-m VIIRS pixel was determined if the crop type was the same in more than 80% 30 m CDL pixels, which was then used to calculate the total area for a single crop type. The cumulative proportion of pure VIIRS pixels was further calculated with the time (DOY) variation of specific phenometrics (Fig. 4). For example, soybean pixels (500-m), where greenup onset appeared, were 9% at DOY 131, and 70% at DOY 164 in South Dakota in 2013 (Fig. 4). In this way, the CDF was calculated for each VIIRS-GLSP phenometrics and each crop type at a state level for a single year. As a result, all CDF curves were produced for six phenometrics, five crop types, and nine years (2013–2021) in each state across the CONUS.

3.1.2. Bridging VIIRS-GLSP to NASS-CPR using exponential models

The VIIRS-GLSP CDF was separately correlated to the NASS-CPR at the temporally neighboring phenological events, which was to bridge VIIRS-GLSP phenometrics to NASS field measured crop growth stages. This phenological match was widely suggested from other efforts (Diao 2020; Gao et al. 2017; Shen et al. 2022), because VIIRS-GLSP

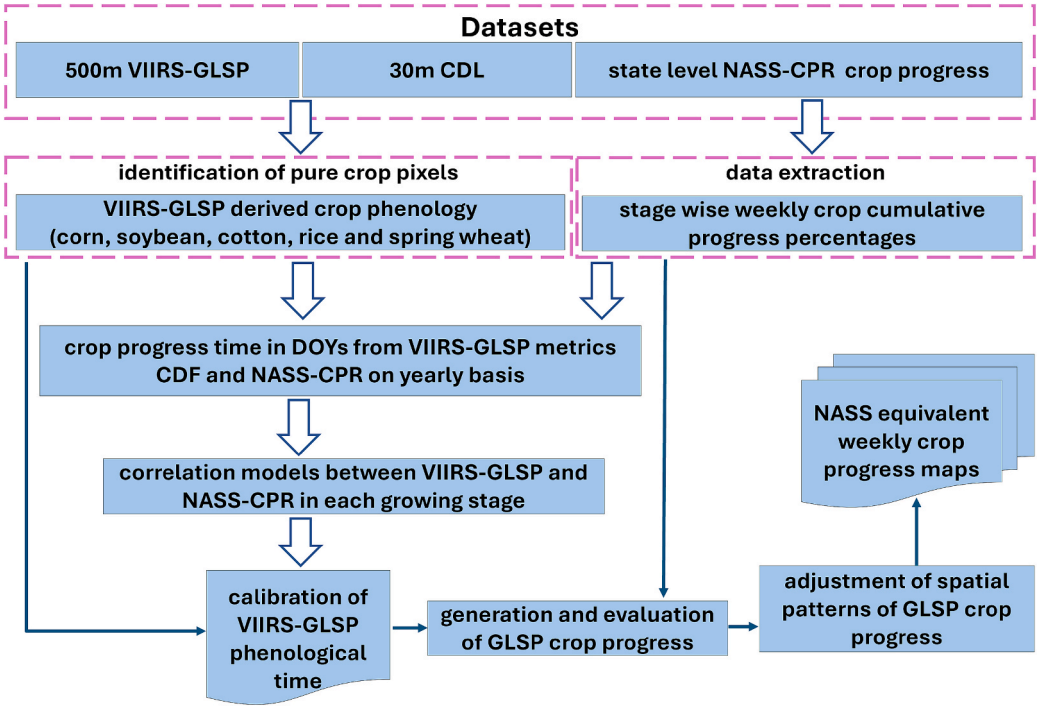

Fig. 3. Workflow for calculating crop progress from VIIRS-GLSP.

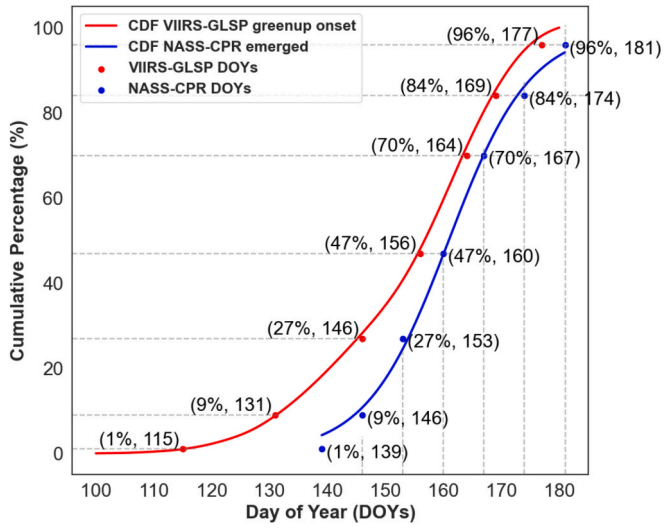

Fig. 4. Matching of cumulative distribution functions of soybean emerged data by NASS-CPR with greenup onset by VIIRS-GLSP in South Dakota in the year 2013.

phenometrics were biophysically different from NASS crop phenology measurements and one VIIRS-GLSP phenometric could correspond to multiple NASS crop growth stages. The details of linkage between VIIRS-GLSP phenometrics and NASS-CPR crop stages were presented in Table 2, indicating their correlation pairs and corresponding definitions of crop growth stages for corn, soybean, rice, spring wheat and cotton. The data pairs were then extracted to generate the correlation models

Table 2
Crop growth stages reported in NASS-CPR data and corresponding VIIRS-GLSP phenology.

VIIRS-GLSP phenometrics	Crop growth stages				
	Corn	Soybean	Rice	Spring wheat	Cotton
greenup onset	planted (seeds sown)				
greenup onset	emerged (some leaves have emerged, and plants are visible)				squaring (small triangular leaf-like structure on the growing tip of the main stem and/or branches.)
maturity onset	silking (silk start emerging from ears)	blooming (bloom appears)	headed (grain bearing part (head) is visible and fully emerged)		setting bolls (one bloom or boll is visible)
maturity onset /senescence onset	dough (soft kernels have dough like matter)	setting pods (pods start developing)			bolls opening (white fibers are visible on at least one boll)
senescence onset/mid-senescence	dented (all kernels are dented with solid ear)				
mid-senescence	mature (ready to harvest soon)	dropping leaves (30–50% yellow leaves)			
dormancy onset	harvested (no green foliage is present and crops are threshed and collected)				

between VIIRS-GLSP phenometrics and NASS-CPR. Specifically, for a given weekly NASS-CPR, we obtained the cumulative percentage of area for a specific growth stage and the corresponding phenological time in DOY. With the same areal percentage, we extracted the corresponding phenological time in DOY from the VIIRS-GLSP CDF (Fig. 4). Thus, the dataset of different phenological times between the two observations were generated for each crop growth stage and crop type from 2013 to 2021. It was assumed that the phenological time difference between VIIRS-GLSP CDF and NASS-CPR at the same areal percentage was due to their discrepancy of biophysical definitions, which could be calibrated or bridged using a correlation model. As a result, all the time differences for the paired NASS-CPR and VIIRS-GLSP phenometrics (Table 2) at a state level were determined from historical phenological data (2013–2021). Because NASS-CPR could be poorly measured at a small percentage of less than 5th percentile or larger than 95th percentile, the corresponding pairs of phenological times were excluded for further analyses. As crop progress could vary from year to year due to varying management practices and changing environmental conditions (Yang et al. 2020), the inter-annual variability in crop progress characterized by VIIRS-GLSP DOYs and NASS-CPR DOYs during 2013–2021 was analyzed and illustrated through boxplots.

The relationships of the phenological times between VIIRS-GLSP phenometrics (independent variable) and NASS-CPR (dependent variable) from 2013 to 2021 were derived using the exponential model (Eq. (1). This model was selected because it performed better than simple linear regression model based on our comparison, in which the result was not shown here. The robustness and generalizability of the developed models were evaluated by applying the leave one year out (LOYO) cross-validation method. The evaluation was measured by calculating the accuracy metrics of root mean square error (RMSE), mean systematic bias (MSB), and R-square (R^2). These metrics were calculated using Eqs. 2–4, where RMSE measures the prediction error, positive or negative MSB values (in days) indicate that VIIRS-GLSP metrics consistently occur later or earlier than NASS data, R^2 represents the proportion of the variance in the NASS-CPR which is predictable from the VIIRS-GLSP estimates.

$$N = a.e^{b.V} \tag{1}$$

Where N and V denote NASS-CPR and VIIRS-GLSP respectively, a and b are model parameters.

$$RMSE = \sqrt{\frac{\sum_{i=1}^{n}(y_i - \hat{y})^2}{n-1}} \tag{2}$$

$$MSB = \frac{1}{n}\sum_{i=1}^{n}(\hat{y}_i - y_i) \tag{3}$$

$$R^2 = 1 - \frac{\sum_{i=1}^{n}(y_i - \hat{y}_i)^2}{\sum_{i=1}^{n}(y_i - \overline{y_i})} \tag{4}$$

Where n is the total number of observations,y_i is the observed value,$\hat{y}_i$ is the predicted value,$\bar{y}$ is the mean of the observed values.

3.2. Calibration of VIIRS-GLSP phenological time for generating GLSP crop progress

The VIIRS-GLSP phenometrics in a given year were used to implement the predictions of NASS-CPR. Specifically, the VIIRS-GLSP phenometrics were first calibrated using the established exponential models (Section 3.12) for each phenological stage and crop type at the corresponding 500-m pixels. This process was referred to as stage-one calibration, which produced spatially distributed crop progress maps with phenological stages equivalent to the NASS-CPR. By aggregating the stage-one calibrated VIIRS-GLSP phenometrics in 500-m pixels at a state level, a weekly NASS-CPR-like crop progress dataset (hereafter referred

to as GLSP crop progress) was produced. As a result, the VIIRS-GLSP phenometrics were able to produce both spatially distributed crop progress at 500-m resolution and weekly GLSP crop progress at a state level (NASS-CPR-like crop progress).

We verified the process of generating weekly GLSP crop progress using VIIRS-GLSP phenometrics in 2022. Note that the data in 2022 were not used for the establishment of calibration models. The weekly GLSP crop progress in 2022 was further used to quantify the bias (difference) with actual NASS-CPR in this year using RMSE, MSB, and R^2.

3.3. Adjustment of spatial pattern in the GLSP crop progress

The GLSP crop progress (section 3.2) was further adjusted at 500-m pixels using the bias with NASS-CPR measurement. This process was to generate a final GLSP crop progress product that was spatially distributed and possessed the same CDF in areal percentage as NASS-CPR at a state level. In other words, NASS-CPR reported a weekly areal percentage for a crop growth stage in a state, but the spatial distribution was unknown. Therefore, the spatial distribution for a 500-m crop growth stage was adjusted using the bias of areal percentage between the GLSP crop progress CDF and the NASS-CPR report separately for each crop type and state on a weekly basis. The bias was reasonable, as uncertainties were inherent in models that converted VIIRS-GLSP phenometrics to ground-observed NASS-CPR, with variations occurring on a weekly basis. Thus, this process was called stage-two calibration.

The stage-two calibration was applied iteratively throughout the entire growing season to adjust the overestimation or underestimation in the GLSP crop progress with the following procedure. The adjustment process for overestimation was illustrated for two consecutive weeks as an example using the following steps (Fig. 5). First, for each NASS-CPR reported DOY (annotation text and point in blue in Fig. 5), the corresponding DOY (annotation text and point in red) from GLSP crop progress (cumulative percentage in CDF) was derived. On a given DOY, GLSP crop progress exhibited a bias with NASS-CPR in cumulative

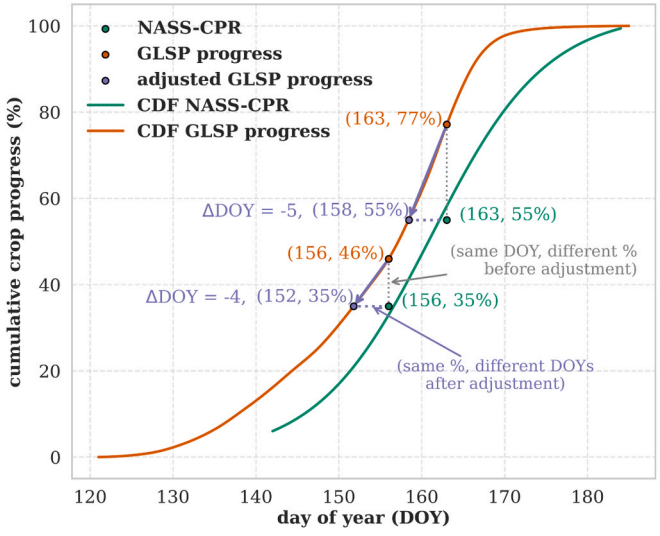

Fig. 5. Conceptual illustration of the CDF-based bias adjustment used to align the calibrated GLSP phenological dates (DOY) with NASS-CPR for a soybean emergence stage in South Dakota (2022). The green and orange curves show the cumulative crop progress from NASS-CPR and GLSP respectively. For selected NASS-CPR reporting dates as examples (green markers), orange points indicate the GLSP cumulative percentage at the same DOYs, and purple points show the adjusted GLSP DOY that matches the NASS-CPR cumulative percentage. Gray vertical segments mark "same DOY, different %" situations, whereas purple dotted horizontal segments and the associated ΔDOY labels denote the time shift applied to the GLSP DOY to obtain "same %, different DOYs" after adjustment. Purple arrows along the GLSP CDF indicate the direction of this correction.

percentage. DOY (annotation text and point in purple) on the GLSP crop progress was then derived. The shaded region between the two CDF curves highlighted the magnitude and direction for bias adjustment of the 500-m GLSP crop progress stage (Fig. 5). The adjustment for individual pixels was illustrated as the following (Fig. 6). Specifically, weekly bias adjustments for overestimation were applied by reassigning the 500-m pixels from the current crop progress stage to either 'nodata' (before planted stage) or a previous stage. Conversely, adjustments for underestimation were made by promoting pixels from 'nodata' or an earlier stage to the current stage. This dynamic adjustment approach ensured that the final weekly maps accurately reflected NASS-CPR while preserving the logical sequence of crop phenological development. The final output consisted of weekly adjusted 500-m crop progress maps representing NASS-CPR equivalent cumulative proportions for different stages within a state.

4. Results

4.1. Inter-annual variation in NASS-CPR and VIIRS-GLSP phenometrics

The VIIRS-GLSP phenometrics and the corresponding NASS-CPR varied inter-annually. The pattern of variation was illustrated with soybean and corn growth stages in South Dakota from 2013 to 2021 (Fig. 7 and Fig. 8). Each boxplot represented the date extracted from VIIRS-GLSP CDF or the corresponding NASS-CPR for establishing calibration models (Fig. 4). The date shifts between VIIRS-GLSP CDF and NASS-CPR varied largely with years and growing stages in soybean (Fig. 7). The VIIRS-GLSP greenup onset showed large late shifts, particularly in 2017 and 2021, in comparison with the NASS-CPR planted dates (Fig. 7a). It was almost overlayed the NASS-CRP emerged dates although the VIIRS-GLSP greenup onset was slightly earlier in 2013 and 2018–2020 but later in 2015–2016 and 2021 (Fig. 7b). The VIIRS-GLSP maturity onset was about 8 days later than the NASS-CPR blooming from 2013 to 2019 while it showed a very short duration in 2020 and 2021 (Fig. 7c). The VIIRS-GLSP maturity onset was about 8 days earlier than the NASS-CPR setting pods in all the years, particularly in 2021 (Fig, 7d). Although the VIIRS-GLSP mid-senescence onset was overall later than the NASS-CPR dropping leaves, it was within the time range of NASS-CPR (Fig. 7e). Lastly, the VIIRS-GLSP dormancy onset was earlier than the NASS-CPR harvest with partial overlaps, but their difference varied largely inter-annually (Fig. 7f).

The boxplots between the VIIRS-GLSP phenometrics and the corresponding NASS-CPR in corn showed similar patterns to those in soybean (Fig. 8). The VIIRS-GLSP greenup onset shifted towards late dates relative to the NASS-CPR planted dates without overlapping except for 2016, 2018 and 2019 (Fig. 8a), which presented large overlaps with NASS-CPR emerged days (Fig. 8b). The VIIRS-GLSP maturity onset showed a minimal overlap with NASS-CPR silking progress and tended to occur about 10 days earlier (Fig. 8c). Additionally, the VIIRS-GLSP senescence onset was about 9 days later and 11 days earlier than the NASS-CPR dough (Fig. 8d) and dented (Fig. 8e) dates respectively with partial overlaps. Both VIIRS-GLSP mid-senescence and dormancy onset occurred earlier than NASS-CPR mature and harvested dates respectively, although interannual variation was evident (Fig. 8f and 8g).

Similar patterns were observed for cotton, rice and spring wheat, which exhibited inter-annual variations in the timing difference between the VIIRS-GLSP phenometrics and NASS-CPR at different growing stages across states, although the details were not presented.

4.2. Models for bridging VIIRS-GLSP phenometrics to NASS-CPR

Calibration models were well established for bridging VIIRS-GLPS phenometrics to the corresponding NASS-CPR across various growth stages, crop types, and states. These models were used to produce the GLSP crop progress. All the model parameters and leave one year out (LOYO) cross validation (R^2 and RMSE scores) were presented in

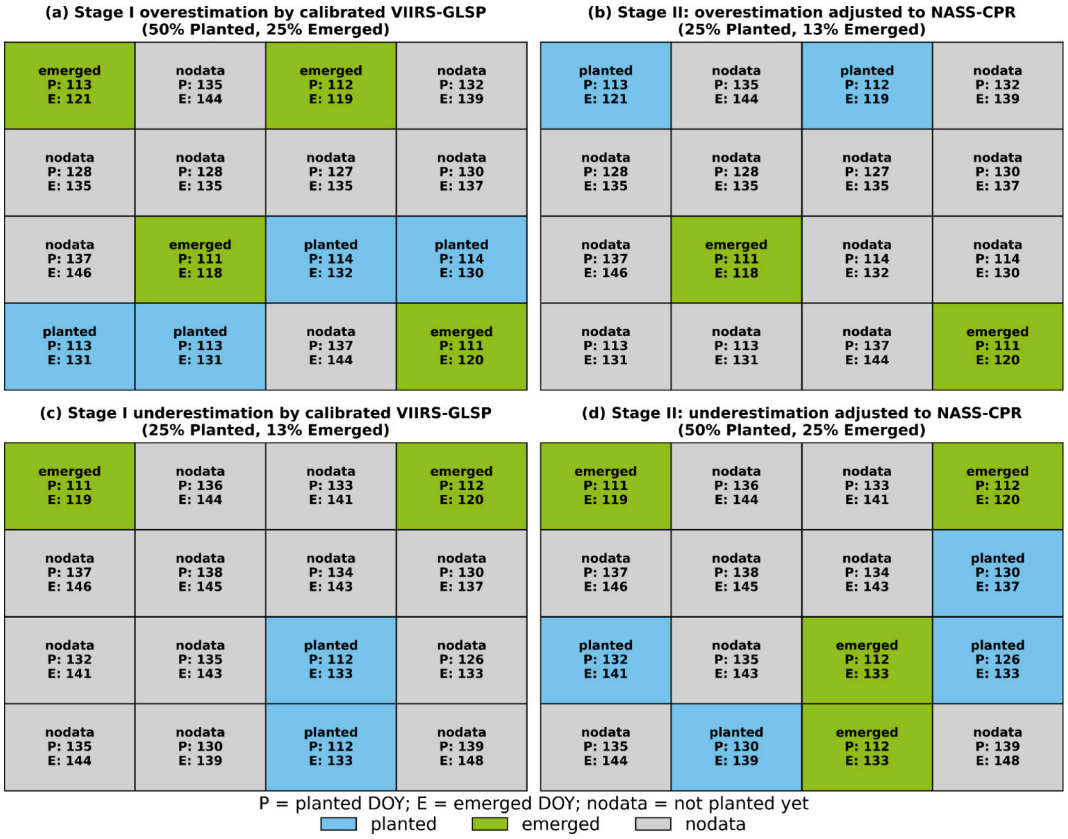

Fig. 6. Illustration of adjusting weekly GLSP crop growth stages in 16 corn pixels using NASS-CPR. The number is the time in day of the year (DOY) of crop growth stages predicted from GLSP phenometrics, where P and E indicate the dates for crop planting and emergence, respectively, in a pixel. The color represents that the GLSP crop growth stage has occurred for plantation (planted) and emergence (emerged) or has not planted yet (nodata) on the date when NASS-CPR reported the crop proportions. In the upper row, it is assumed that NASS-CPR reports 25% planted and 13% emerged areas on DOY 125. However, the GLSP crop growth stage predicted using stage-one calibration shows 50% planted and 25% emerged areas on DOY 125 (6a), which overestimates the crop progress. Thus, the areal bias in GLSP crop progress is adjusted to match the NASS-CPR, which results in the spatial pattern with the same areal percentage as NASS-CPR (6b). In the bottom row, it is assumed that NASS-CPR reports 50% planted and 25% emerged areas on DOY 125. However, the GLSP crop growth stage predicted using stage-one calibration shows 25% planted and 13% emerged areas on DOY 125 (6c), which underestimates the crop progress. Thus, the areal bias in GLSP crop progress is adjusted to match the NASS-CPR, which results in the spatial pattern with the same areal percentage as NASS-CPR (6d).

Tables S1–S5, which were separately established for five crop types (soybean, corn, cotton, rice, and spring wheat) across various states within CONUS (Fig. 2).

For soybean and corn, the models for converting the VIIRS-GLSP phenometrics to the corresponding NASS-CPR were overall significant (p-value < 0.05) with across the states average R^2 ranging from 0.41 and 0.43 for soybean and corn planted stages to 0.86 and 0.88 for the soybean blooming and leaf dropping stages and the corn silking stage. The models between the VIIRS-GLSP phenometrics and the NASS-CPR were further verified using soybean and corn growths in South Dakota (Figs. 9 and 10), as an example. Based on the NASS-CPR observations and the GLSP crop progress from 2013 to 2021, the LOYO R^2 was (1) 0.2 and 0.29 for soybean and corn planted stages derived from the VIIRS-GLSP greenup onset, respectively; (2) 0.39 and 0.49 for soybean and corn emerged stages derived from the VIIRS-GLSP greenup onset, respectively; (3) 0.7 and 0.78 for soybean blooming and pod-setting stages and 0.72 for corn silking stage derived from the VIIRS-GLSP maturity onset; (4) 0.7 and 0.81 for corn dough and dented stages, respectively, derived from the VIIRS-GLSP senescence onset; (5) 0.89 and 0.88 respectively for soybean leaf dropping and the corn mature stages derived from the VIIRS-GLSP mid-senescence, and (6) 0.63 and 0.74 respectively for soybean and corn harvesting dates derived from the VIIRS-GLSP dormancy onset.

For cotton, the models also demonstrated the strong correlation between the GLSP crop progress and the NASS-CPR measurements. NASS-CPR showed an average LOYO R^2 of 0.71 with the planted dates derived from the VIIRS-GLSP greenup onset for most states except California, Kansas, Missouri, and Oklahoma. The average LOYO R^2 was 0.57 for cotton squaring stage derived from the VIIRS-GLSP greenup onset and 0.67 for the cotton bolls setting stage derived from the VIIRS-GLSP maturity onset across the states except Oklahoma. Similarly, an average LOYO R^2 of 0.67 was observed for the cotton bolls opening stage derived from the VIIRS-GLSP senescence onset in all states. The NASS-CPR harvesting dates for cotton were correlated to the derivation of the VIIRS-GLSP dormancy onset, with an average LOYO R^2 value of 0.67 for all states except Kansas and Oklahoma.

For rice and spring wheat that were mainly distributed in six states (Fig. 2), the GLSP crop progress also exhibited strong correlations with the NASS-CPR measurements. Their average LOYO R^2 was 0.78 for the planted stage of rice except Missouri and Texas states and 0.36 for spring wheat. The R^2 was 0.65 and 0.53 respectively for both rice and spring wheat emergence stages. The NASS-CPR headed stage of both rice and spring wheat were strongly correlated to the derivation from VIIRS-GLSP maturity onset across the states with an average R^2 of 0.82 and 0.67 respectively. Similarly, the NASS-CPR harvesting dates for rice and spring wheat except Minnesota and South Dakota were moderately correlated to the derivations from VIIRS-GLSP dormancy onset, with an average R^2 of 0.54 and 0.5, respectively.

4.3. *Evaluating the model application for estimating GLSP crop progress*

The GLSP crop progress, derived from the VIIRS-GLSP phenometrics

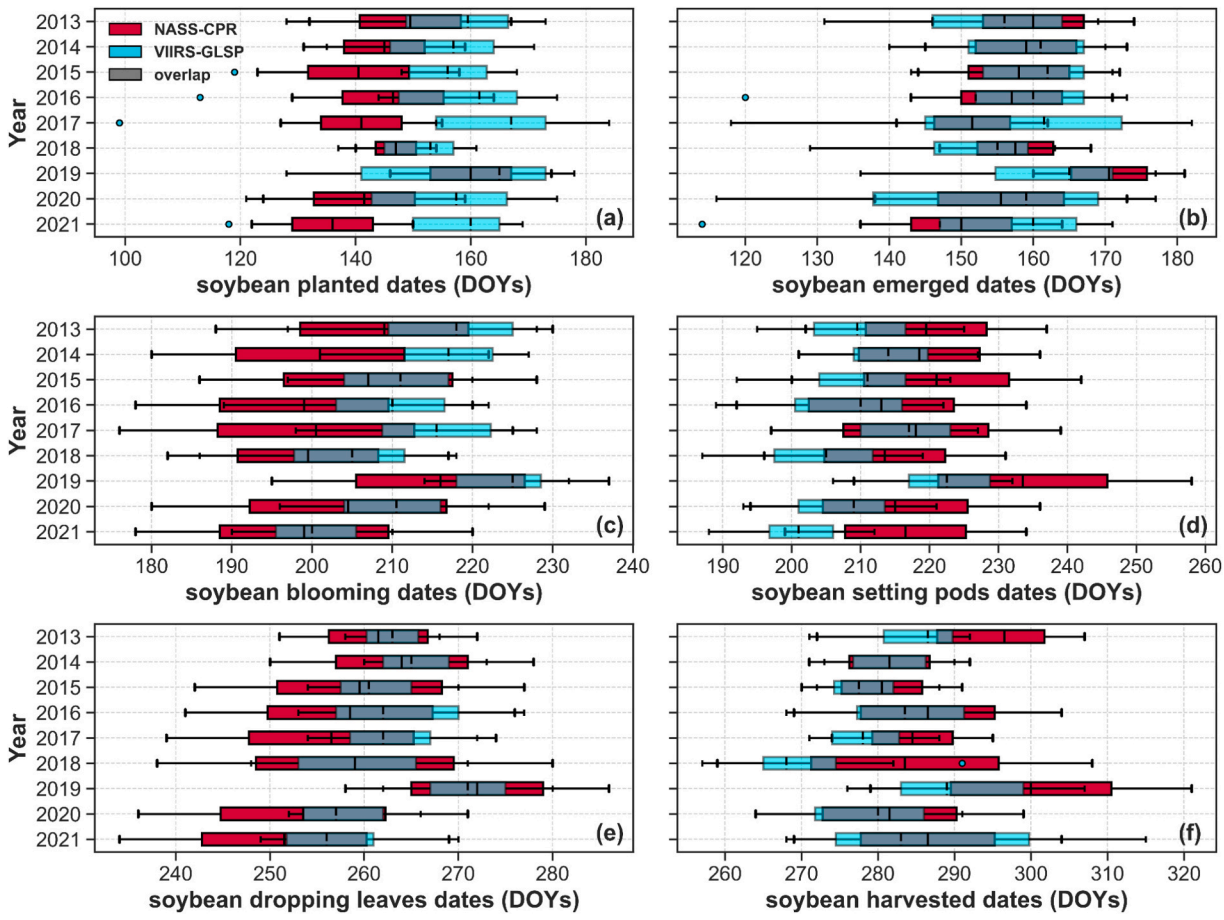

Fig. 7. Inter-annual variation of soybean growth progress in South Dakota from 2013 to 2021 as reported by NASS and derived from VIIRS-GLSP (a) planting and greenup onset (b) emergence and greenup onset (c) blooming and maturity onset (d) setting pods and maturity onset (e) dropping leaves and mid-senescence onset (f) harvested and dormancy onset.

after applying the stage-one calibration models (Tables S1-S5 in supplementary file) at 500-m pixels, was able to closely track the crop progress from the NASS-CPR although the accuracy varied with crop stages across various states. The application of stage-one calibration models for bridging the VIIRS-GLSP to the NASS CPR was illustrated using data in 2022 in South Dakota (Fig. 11 and Fig. 12). The statistical parameters of correlations for soybean and corn were presented here in Tables 3 and 4 respectively. Note that the VIIRS-GLSP in 2022 was not used for the establishment of the calibration models.

The GLSP crop progress showed close alignments with the NASS-CPR over various crop growing stages, while the original VIIRS-GLSP phenometrics presented a large departure from the NASS-CPR. Specifically, the original greenup onset CDF failed to capture the NASS-CPR planted and emerged stages for both soybean and corn (Fig. 11a-b and 12a-b). For example, the original VIIRS-GLSP CDF curves (red color) based on greenup onset and dormancy onset tended to overestimate crop emerged and harvested progress. Likewise, the VIIRS-GLSP CDF of maturity onset overestimated soybean setting pods and corn silking stages. Similarly, senescence onset and mid-senescence largely overestimated corn dented and mature stages respectively, whereas the maturity onset and senescence onset underestimated soybean blooming and corn dough stages respectively. In contrast, the GLSP crop progress aligned well with NASS-CPR data, showing slight overestimation during early and later periods. Although the GLSP crop progress derived from greenup onset overestimated NASS-CPR for the early planted and emerged stages but exhibited less bias in their later stages. The GLSP crop progress for emergence tended to follow closely the NASS-CPR for the soybean emergence although a small shift existed. Additionally, the GLSP crop progress showed minimal bias compared to NASS-CPR data for soybean stages in blooming (Fig. 11c), setting pods (Fig. 11d), and dropping leaves (Fig. 11e), as well as corn stages in silking (Fig. 12c) and mature (Fig. 12f).

Similarly, the GLSP crop progress highlighted the effectiveness in predicting the NASS-CPR for various phenological stages in all the crop types (soybean, corn, cotton, rice, and spring wheat) in each individual state (Figs. S1–S51). The temporal pattern of the GLSP crop progress was comparable to the NASS-CPR although the bias varied with crop types, phenological stages, and states.

Statistical analysis further revealed the discrepancy and similarity of the GLSP crop progress with the NASS-CRP in 2022. For soybean (Table 3), the GLSP crop progress for planted and emerged stages showed a RMSE ranging from 3 to 11 days across the states. It was earlier than the NASS-CPR with a MSB of −2 to −10 days in Minnesota, Missouri, North Dakota, and South Dakota, but later in other states with an MSB ranging from 1 to 6 days. The GLSP crop progress for the blooming and setting pods stages presented a RMSE less than 6 days in most states but 7–13 days in Illinois, Michigan, North Dakota, and Ohio. It was later than the NASS-CPR measurement with a MSB ranging from 2 to 12 days in most states except for Illinois, Iowa, and Kansas. The GLSP crop progress for dropping leaf stage showed a RMSE ranging from 1 to 8 days across the states, which was 1–8 days later than the NASS-CPR. Finally, the GLSP crop progress for harvested stage was generally 2–10 days later with a RMSE less than 10 days.

Compared with the NASS-CPR for corn (Table 4), the GLSP crop progress for planted and emerged stages showed a MSB from −2.25 to −10.38 and 0.2 to −13 days, respectively. The RMSE was around 7 days,

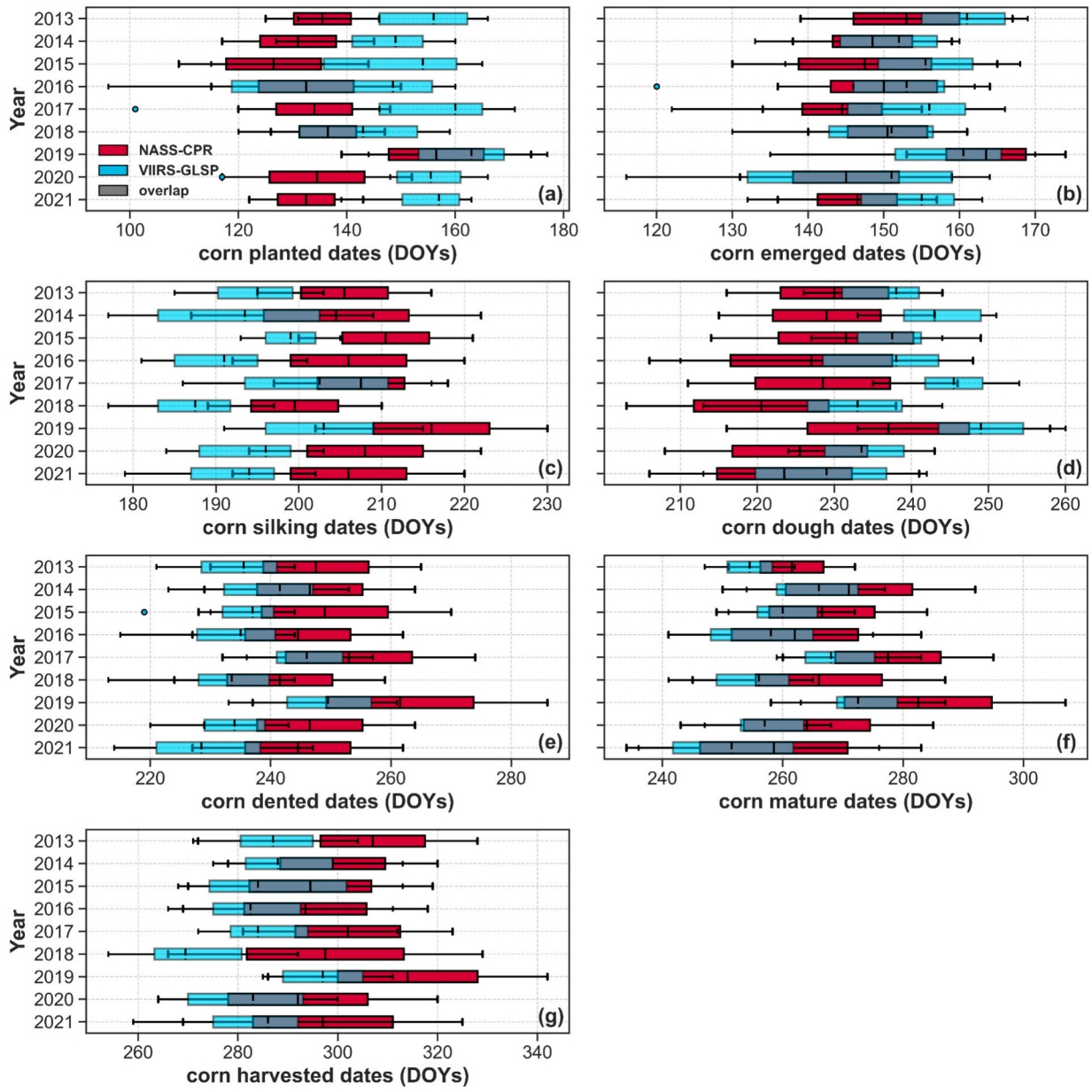

Fig. 8. Inter-annual variation of corn growth progress in South Dakota from 2013 to 2021 as reported by NASS and derived from VIIRS-GLSP (a) planting and greenup onset, (b) emergence and greenup onset, (c) silking and maturity onset, (d) dough and senescence onset, (e) dented and senescence onset, (f) mature and mid-senescence phase, and (g) harvested and dormancy onset.

with a higher RMSE in Illinois, Indiana, Missouri, and North Dakota. The GLSP crop progress for corn silking stage presented higher accuracy with RMSE $<$ 5 days in most states although it was around 5 days earlier in most states while 5 days later in Indiana, Kentucky, and Michigan. The GLSP crop progress for corn dough and dented stages showed a RMSE less than 10 days in most states but 10–13 days in Kentucky, Michigan and Ohio, which was around 8 days earlier than NASS-CPR in most states. For the mature stage, the GLSP crop progress had a RMSE of 9 days and an MSB $<$ 9 days in all states except Ohio. For the harvested stage, the GLSP crop progress was 1—15 days later with RMSE ranging from 4 to 15 days.

Compared with the NASS CPR in 2022, similarly, the GLSP crop progress showed compatibility in five cotton stages and six stages of rice and spring wheat (Tables S6-S8). The GLSP crop progress in cotton planted and squaring stages was 5 days later across the states, with a RMSE of around 8 days in the planted stage (except for California, Kansas and Missouri) and 7 days in the squaring stage (except for Kansas, Oklahoma, Texas and Virginia). The GLSP crop progress revealed a RMSE of 8 days in the cotton bolls setting stage in all states except for Tennessee and Texas states, whereas it was 9 days on average in the cotton bolls opening stage in all states. The GLSP crop progress was 5 days later in the boll setting stage but 5 days earlier in the boll opening stage than the NASS-CPR. Less discrepancies were observed for the cotton harvested stage with an average RMSE of 6 days except for South Carolina state. The cotton harvested stage from the GLSP crop progress was earlier than the NASS-CPR observations with an MSB of 2 days on average.

The progress for four rice and spring wheat stages (planted, emerged, heading, and harvested) in the states (Arkansas, California, Louisiana, Mississippi, Missouri and Texas for rice, and Idaho, Minnesota, Montana, North Dakota, South Dakota and Washington for spring wheat) was estimated from the calibrated models of VIIRS-GLSP phenometrics with a RMSE less than 8 days for all stages except the rice harvested stage. The GLSP crop progress for the planted and emerged stages in rice

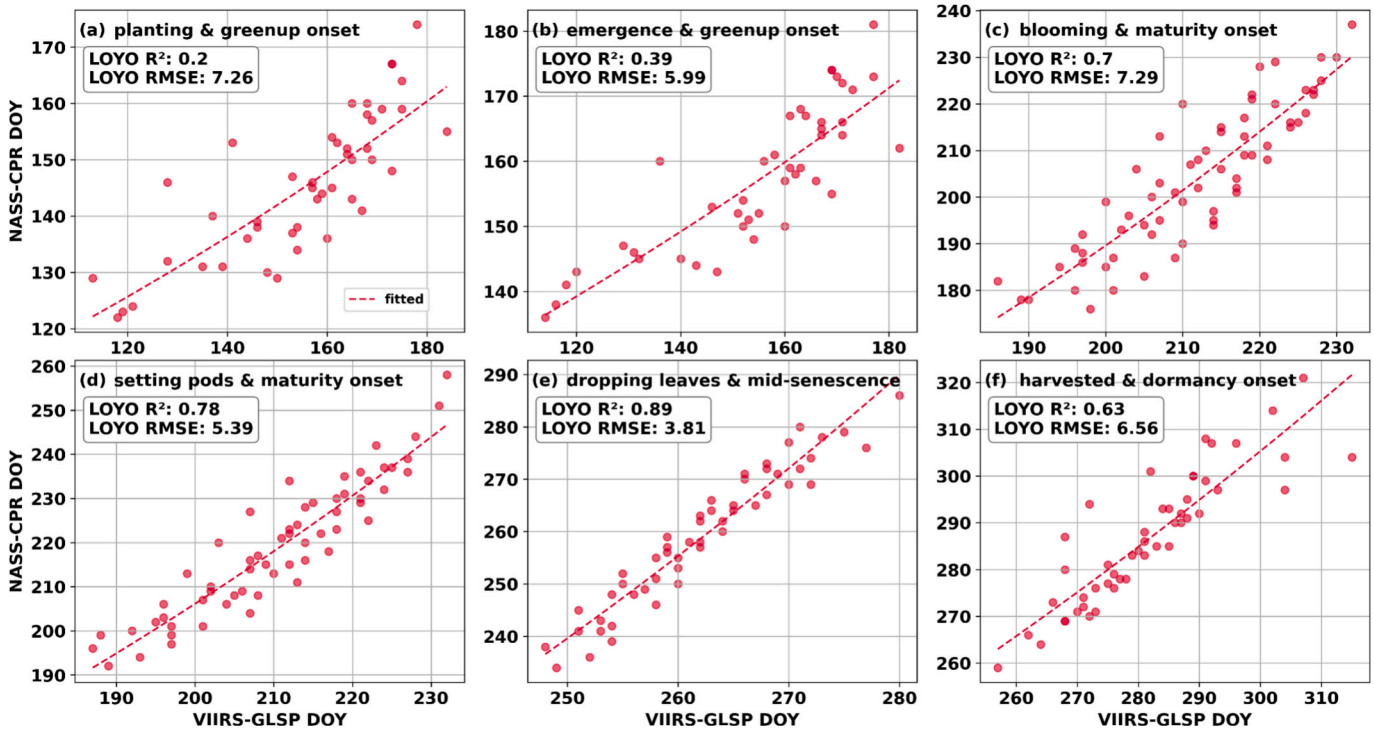

Fig. 9. Scatterplots of the soybean NASS-CPR and VIIRS-GLSP derived crop progress from 2013 to 2021 in South Dakota, showing the model development result of leave one year out (LOYO) cross validation for estimated GLSP crop progress.

and spring wheat presented a RMSE of around 6 days in all states except for the rice planted stage in Louisiana and Missouri. In most states and growth stages, the GLSP crop progress was slightly earlier than the NASS-CPR data with a MSB less than 2 days on average, whereas it was later for rice in Mississippi and Texas and for spring wheat in Montana and South Dakota. The GLSP crop progress for heading stage of both crops indicated a RMSE of around 5 days, where rice heading progress was generally 2 days later than the NASS-CPR measurements while the spring wheat heading progress was 1 day earlier in most states. The GLSP crop progress for the harvested stage in rice and spring wheat had a RMSE of less than 10 days except for rice in California and Texas. For both crops, the estimates were earlier than the NASS-CPR, with MSB values of 9 days for rice and 5 days for spring wheat.

4.4. *Spatial patterns of the GLSP crop progress*

The weekly GLSP crop progress offered spatial distribution with distinct regional and temporal patterns. The weekly interval was to align with the temporal frequency of NASS CPR although the GLSP crop progress could be mapped at any temporal resolution. Fig. 13 presented an example in the soybean field exhibiting the spatial differences between the VIIRS-GLSP greenup onset and the GLSP crop progress for planted stage and emerged stage on DOY 156 in 2022. Specifically, Fig. 13a showed the spatial patterns of VIIRS-GLSP greenup onset for soybean during the 2022 growing season in South Dakota, indicating that soybean experienced later greenup onset in the northern parts of South Dakota. Fig. 13b displayed the GLSP crop progress for soybean planted and emerged stages that occurred in most soybean fields on DOY 156.

Fig. 14 and Fig. 15 presented the spatiotemporal patterns of the GLSP crop progress for soybean and corn growth stages across the CONUS Corn Belt during 2022. To visualize the temporal progression over whole growing season, the GLSP crop progress was shown for every third week, beginning from week 20 (DOY 142) to week 44 (DOY 310) in 2022. Evidently, corn was planted earlier compared to soybean (Fig. 14a and Fig. 15a), where the planted area for corn was larger than that of soybean on DOY 142. Further, a clear southwest-to-northeast progression pattern of crop growth stages was observed for both soybean and corn. For soybean on DOY 163 (Fig. 14b), planted areas were shown in the northeastern parts of North Dakota (ND), South Dakota (SD), Iowa (IA), and Ohio (OH), while emerged areas were displayed in the southwestern parts of these states. This spatial progression was consistent for later growth stages, such as blooming, setting pods, dropping leaves, and harvest (Fig. 14). For corn, a similar southwest-to-northeast progression pattern was evident. Fig. 15d- 15h depicted the advancement of silking, dough, dented, and mature stages. Specifically, the eastern parts of states like SD and Nebraska (NE), as well as the southwestern regions of Minnesota (MN), IA, and Illinois (IL), exhibited earlier progress in these stages compared to the northeastern parts of MN, IA, and IL, and the western regions of Indiana (IN), Michigan (MI), and OH.

The spatial distribution of the adjusted GLSP crop progress was produced every week for five crop types across the CONUS. The result was illustrated using an example in South Dakota. Fig. 16 illustrates the bias in the GLSP crop progress relative to the NASS-CPR reported progress and the bias adjustment based on soybean progress estimates in South Dakota across two consecutive weeks. The maps demonstrated the necessary adjustments to align GLSP crop progress with NASS-CPR based on the procedure explained in Fig. 5 and Fig. 6. In Fig. 16a (first row), soybean crop progress on DOY 149 (2022) showed that there were 63% planted and 28% emerged (left panel) in the GLSP crop progress, which led to spatially biased pixels in comparison with the NASS-CPR (center panel). After the bias adjustment, the adjusted GLSP crop progress matched the NASS-CPR values that had 61% planted and 16% emerged areas (right panel in Fig. 16a). Similarly, Fig. 16b (second row) presents maps on DOY 156, where GLSP crop progress initially estimated 93% planted and 46% emerged areas, which were adjusted to align with NASS-CPR values of 77% planted and 35% emerged areas. The bias maps specifically indicated the spatial distribution of pixels where the GLSP crop progress was deviated from NASS-CPR on a given day of year. The pixels adjusted GLSP crop progress exhibited stage-wise proportions that aligned with NASS-CPR after the biased pixels were

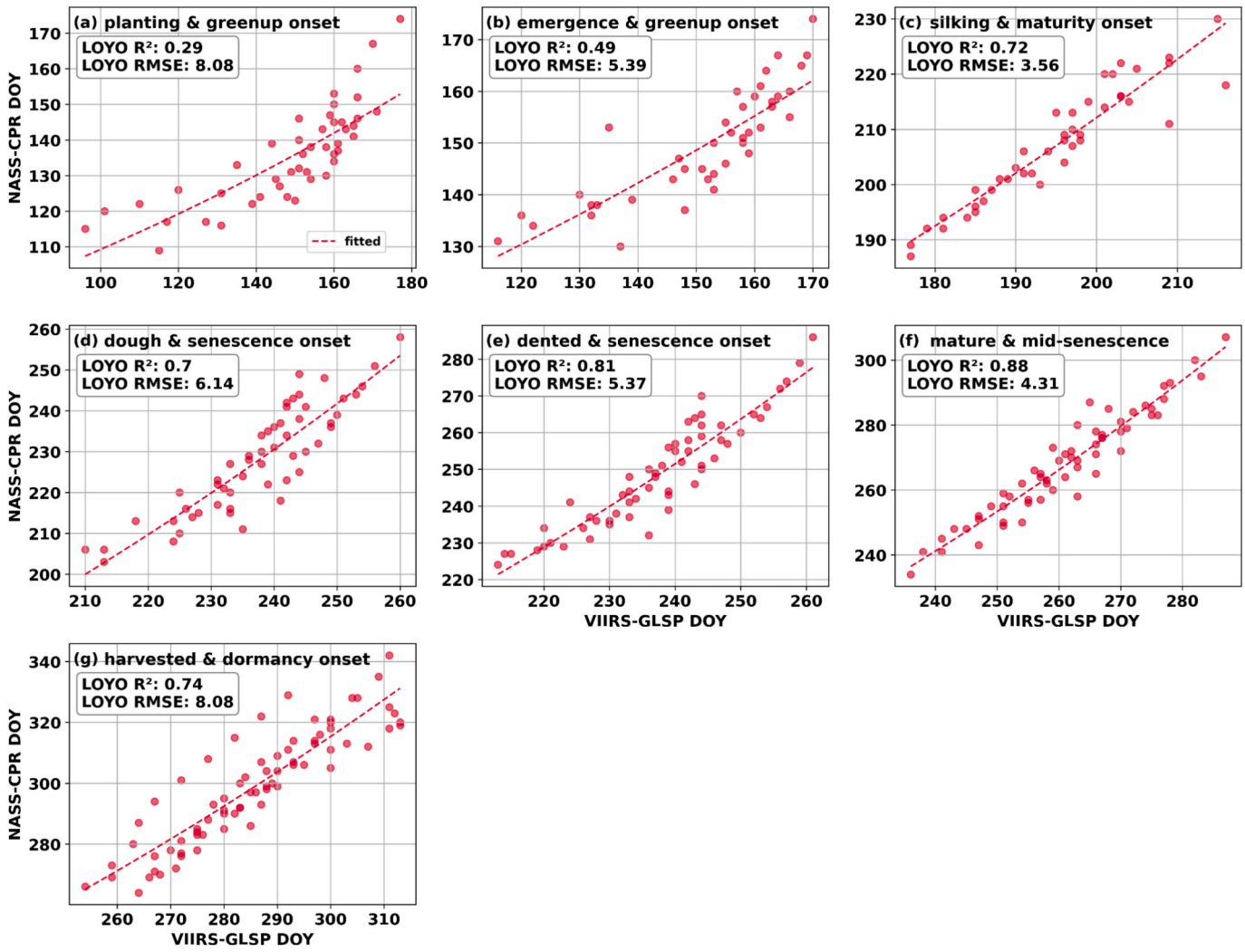

Fig. 10. Scatterplots of the corn NASS-CPR and VIIRS-GLSP derived crop progress from 2013 to 2021 in South Dakota, showing the model development result of leave one year out (LOYO) cross validation for estimated GLSP crop progress.

adjusted by shifting progress backward or forward. The process ensured logical and consistent transition of crop stages while preserving spatial consistency with NASS-CPR.

5. Discussion

This study demonstrated the potential of VIIRS-GLSP phenometrics for effectively tracking the progression of crop development stages at a weekly interval, as reported in the NASS crop progress reports (NASS-CPR). We proposed a two-stage calibration framework to monitor crop progress based on long-term VIIRS-GLSP product and NASS-CPR data. In the first stage, we established a set of correlation models that bridged the VIIRS-GLSP phenometrics to the NASS-CPR, which produced the GLSP crop progress. This calibration was necessary because VIIRS-GLSP phenometrics were determined with totally different biophysical definitions from field-based NASS CPR measurements as described in Tables 1 and 2, even though they were closely correlated (Diao 2020; Gao et al. 2017; Shen et al. 2022). Their correlation models exhibited strong significance with a mean R^2 value greater than 0.7 for all crop stages and states, particularly in the growth stages of soybean blooming, corn silking stage, cotton boll setting and opening stages, and rice and spring wheat heading stages. In the second stage, the modeled GLSP crop progress was adjusted using weekly NASS-CPR percentages to ensure consistency with field-based observations. The adjusted GLSP crop progress not only provided percentage-format crop progress at a state-level that was equivalent to NASS-CPR data but also produced spatial distributions for each crop phenological stage at 500-m pixels. The spatial distribution pattern offered significant enhancement for operationally reported NASS-CPR.

A key contribution of this study is the development of a scalable and operational framework for translating VIIRS-GLSP phenometrics into weekly crop progress estimates directly comparable to NASS-CPR across CONUS. In contrast to previous studies that emphasized improving field-scale crop (mainly corn and soybean) phenology detections through computationally intensive multi-sensor fusion at local areas and evaluating satellite-derived phenometrics using NASS-CPR (Gao et al. 2017; Shen et al. 2022; Shen et al. 2023), our study focused on the determination of NASS-CPR crop growth stages (corn, soybean, rice, spring wheat, and cotton) using operationally produced NASA VIIRS phenology product, and the estimation of NASS-CPR crop growth stages for each VIIRS pixel using VIIRS phenometrics across CONUS. Further, because VIIRS-GLSP has been operationally produced since 2013 (Zhang et al. 2024), our method offers an operational framework that statistically translates VIIRS-GLSP phenometrics to NASS-CPR crop growth stage to produce weekly and pixel-based crop progress over a large region. To our knowledge, this is the first operational and CONUS-scale framework capable of generating NASS-equivalent weekly crop progress using VIIRS-GLSP product.

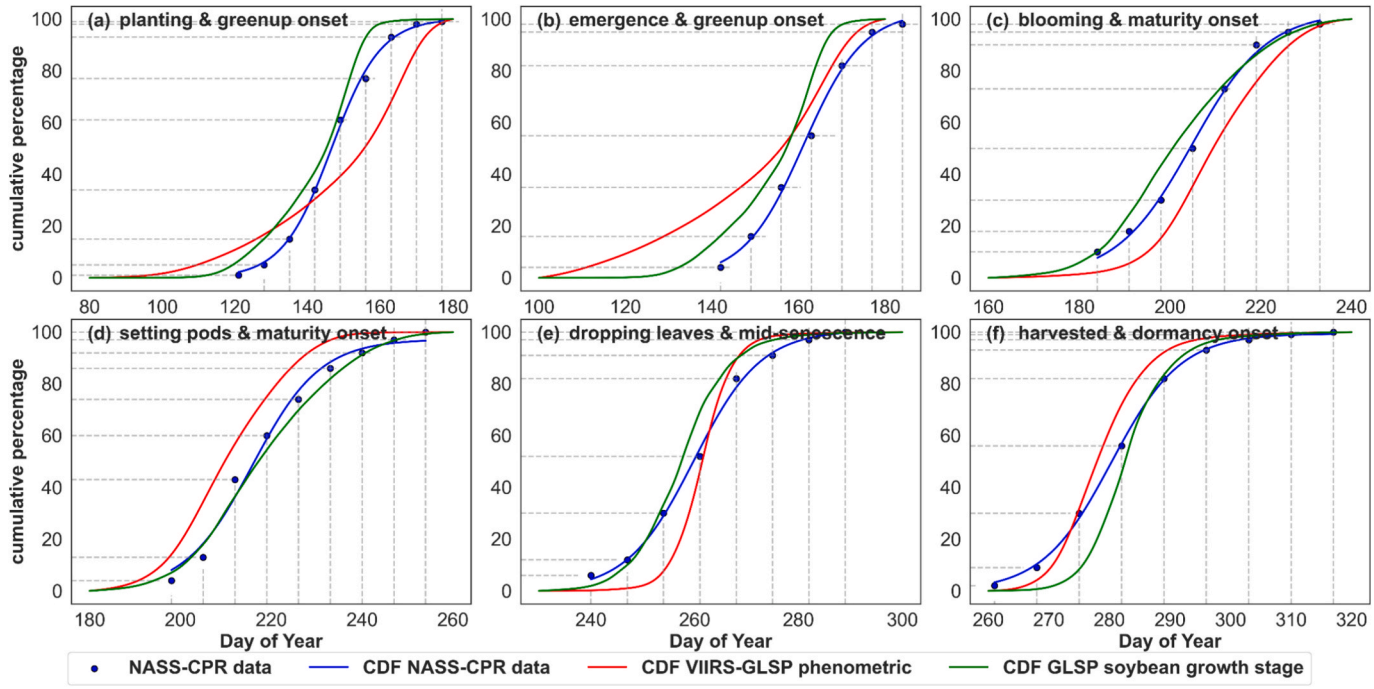

Fig. 11. Comparison of the GLSP crop progress for soybean growth stages with original VIIRS-GLSP phenometrics and NASS-CPR in South Dakota in 2022.

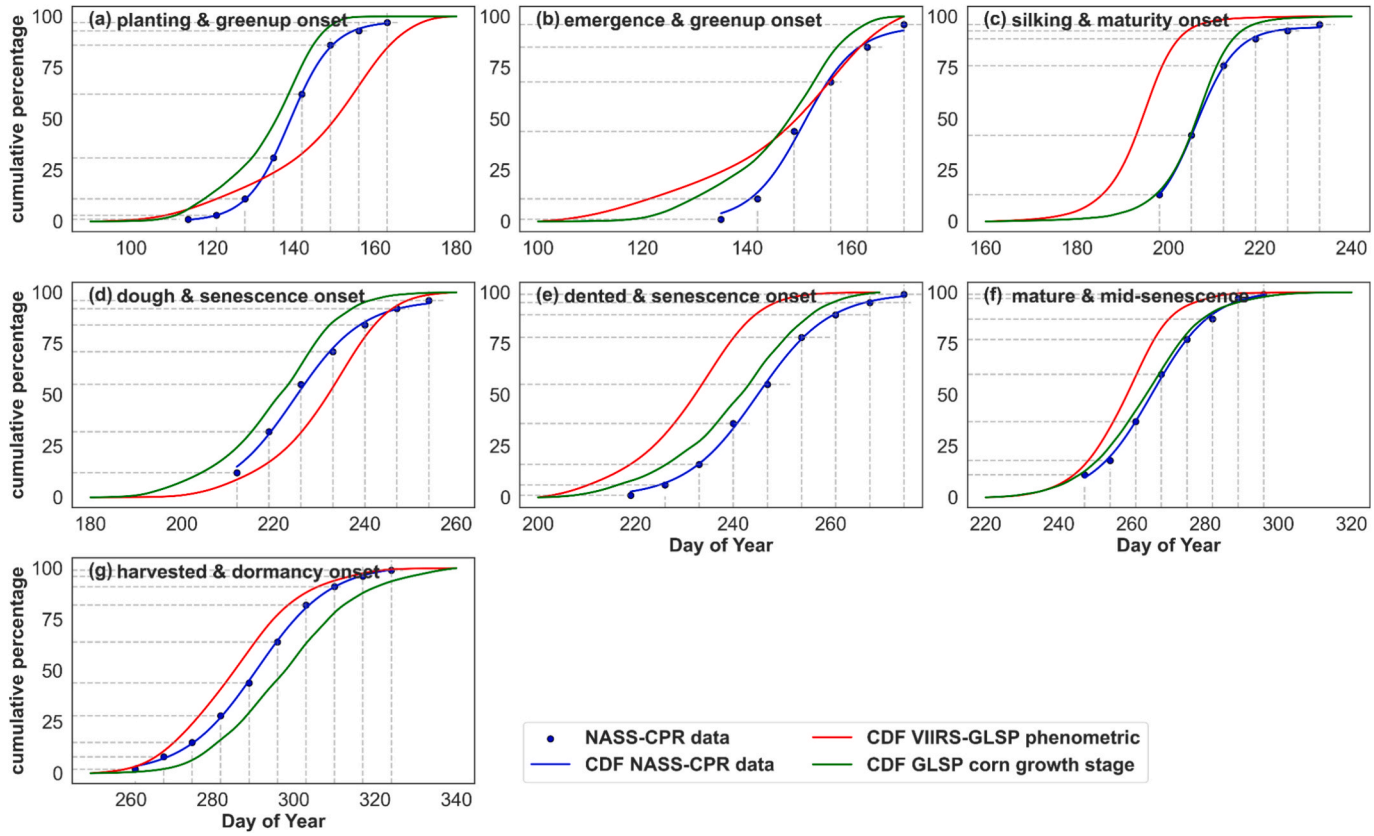

Fig. 12. Comparison of the GLSP crop progress for corn growth stages with original VIIRS-GLSP phenometrics and NASS-CPR in South Dakota in 2022.

The VIIRS-GLSP phenometrics were consistently correlated with NASS-CPR although they were biophysically different. They showed coincidentally interannual variations associated with fluctuations in temperature, precipitation, and field management practices. For instance, cooler springs, as observed in 2014 (USDA 2015) and 2019 (USDA 2020), led to delayed planted stage and slower early-stage growth of soybean and corn in the CONUS Corn Belt as observed by NASS-CPR (Fig. 7a-7b and Fig. 8a-8b), resulting in late emergence and subsequent stages. Conversely, warmer than average spring temperatures in 2017 (USDA 2018) advanced the planted and subsequent

Table 3
Model evaluation metrics for soybean growth stages for the years 2022 across the states. Note that for crop phenological stage in a state where model performed worse, the accuracy metrics were filled with "NA".

NASS-CPR vs GLSP crop progress in soybean stages																		
States	planting			emergence			blooming			pods setting			dropping leaves			harvest		
	R^2	RMSE	MSB	R^2	RMSE	MSB	R^2	RMSE	MSB	R^2	RMSE	MSB	R^2	RMSE	MSB	R^2	RMSE	MSB
Illinois	0.38	11.05	0.86	0.14	11.11	4.33	0.77	7.64	−6.38	0.48	12.99	−10.44	0.23	8.66	7.80	0.66	7.01	6.17
Indiana	0.12	11.20	−1.17	0.38	7.77	3.60	0.93	3.78	3.43	0.97	2.81	2.13	0.76	5.92	5.67	0.46	10.31	10.00
Iowa	0.61	6.21	2.20	0.67	5.67	4.20	0.89	4.58	−2.14	0.93	3.68	−1.00	0.93	2.61	2.40	0.56	7.94	7.67
Kansas	0.93	4.84	−0.11	0.94	3.89	0.63	0.93	3.66	−2.57	0.89	5.34	−4.50	0.99	1.20	0.29	0.87	5.70	5.50
Kentucky	0.58	13.10	5.90	0.54	10.86	6.88	0.90	5.73	3.67	0.93	4.75	1.67	0.96	2.73	1.14	NA	NA	NA
Michigan	0.96	2.35	1.17	0.92	3.32	1.00	0.64	8.38	7.86	0.59	9.02	8.43	0.82	5.95	2.57	0.92	4.57	2.13
Minnesota	0.41	7.60	−7.00	0.79	5.43	−4.83	0.95	2.68	2.50	0.95	3.21	2.86	0.85	3.00	2.50	0.73	4.06	4.00
Missouri	0.90	5.60	−2.00	0.68	9.06	−5.25	0.87	5.74	5.25	0.92	5.02	4.56	0.64	7.14	7.00	0.76	6.85	6.29
Nebraska	0.41	7.58	7.40	0.77	5.73	4.17	0.92	4.05	1.57	0.83	4.98	3.83	0.97	2.24	1.33	0.88	4.18	3.83
North Dakota	NA	NA	NA	NA	NA	NA	0.36	9.56	9.00	0.64	7.20	6.83	0.81	4.27	1.00	0.70	5.46	5.40
Ohio	0.78	5.55	0.17	0.79	6.38	−1.86	0.05	13.62	12.43	0.59	11.58	11.33	0.56	7.93	7.83	0.20	10.68	10.33
South Dakota	0.77	5.73	−5.17	0.60	6.29	−6.00	0.95	3.18	−1.57	0.96	2.27	1.17	0.93	3.27	−1.00	0.84	3.97	2.20
Wisconsin	0.89	3.96	3.33	0.90	3.87	3.33	0.75	7.03	6.86	0.91	4.74	4.25	0.86	2.96	2.75	0.78	5.64	4.83
Average	0.65	7.06	0.47	0.68	6.62	0.85	0.76	6.13	3.07	0.81	5.97	2.39	0.79	4.45	3.18	0.7	6.36	5.7

Table 4
Model evaluation metrics for corn growth stages for the years 2022 across the states. Note that for crop phenological stage in a state where model performed worse, the accuracy metrics were filled with "NA".

	NASS-CPR vs GLSP crop progress in corn stages																				
	planting			emergence			silking			dough			dented			mature			harvest		
	R^2	RMSE	MSB	R^2	RMSE	MSB	R^2	RMSE	MSB	R^2	RMSE	MSB	R^2	RMSE	MSB	R^2	RMSE	MSB	R^2	RMSE	MSB
Illinois	0.25	10.32	−8.83	0.20	7.02	−3.75	0.81	3.39	−2.50	0.76	8.83	1.11	0.68	9.08	−2.75	0.82	6.75	0.25	0.64	9.64	9.00
Indiana	0.39	9.37	−8.17	0.15	9.14	−6.40	0.94	2.37	2.00	0.67	8.03	7.86	0.86	5.29	5.14	0.75	8.08	7.25	0.27	15.46	14.89
Iowa	0.59	6.32	−6.00	0.72	5.25	−3.20	0.94	2.32	−1.00	0.63	7.28	6.67	0.82	5.92	5.29	0.36	9.57	9.50	0.25	13.93	13.88
Kansas	0.92	5.03	−0.67	0.86	5.94	−3.75	0.81	7.85	−7.11	0.76	8.86	−8.44	0.77	7.73	−5.75	0.95	3.50	−1.50	0.98	2.58	1.33
Kentucky	0.22	14.18	−10.38	0.31	11.64	−8.43	0.95	3.43	2.00	0.68	10.25	8.78	0.57	10.47	7.13	0.78	7.56	2.13	0.86	6.75	3.56
Michigan	0.88	2.69	−2.25	0.88	3.38	−2.20	0.68	4.44	4.25	0.11	13.17	13.00	0.29	11.81	11.43	0.75	7.96	6.38	0.60	10.08	8.63
Minnesota	0.05	9.64	−9.40	0.42	5.96	−5.50	0.88	2.74	−0.50	0.85	4.58	2.67	0.93	3.27	2.33	0.41	7.62	7.60	0.02	11.83	11.67
Missouri	0.33	11.43	−10.00	0.01	11.87	−9.00	0.94	2.89	−2.67	0.93	3.80	3.29	0.85	4.67	0.83	0.85	5.49	2.71	0.88	7.01	3.60
Nebraska	0.91	3.54	−0.50	0.87	3.52	−0.80	0.85	4.56	−3.50	0.66	8.16	−7.14	0.94	2.86	−2.50	0.94	4.05	2.38	0.72	9.55	8.78
North Dakota	NA	NA	NA	NA	NA	NA	0.83	5.81	0.00	0.89	4.57	0.86	0.95	3.27	−1.00	0.89	3.98	3.83	NA	NA	NA
Ohio	0.47	8.71	−6.50	0.54	8.07	−4.83	0.61	6.20	5.60	0.28	11.89	11.71	0.68	9.10	9.00	0.23	14.04	13.50	NA	NA	NA
South Dakota	0.56	6.54	−6.00	0.21	6.95	−5.75	0.74	5.04	−3.40	0.68	6.81	−6.33	0.82	5.90	−5.43	0.96	2.42	−2.17	0.65	8.25	8.00
Wisconsin	0.76	5.83	−5.00	0.94	2.49	0.20	0.97	2.00	0.33	0.54	9.46	8.57	0.61	8.78	8.29	0.48	8.66	8.33	0.90	4.52	1.00
Average	0.53	7.8	−6.14	0.51	6.77	−4.45	0.84	4.08	−0.5	0.65	8.13	3.28	0.75	6.78	2.46	0.71	6.9	4.63	0.62	9.05	7.67

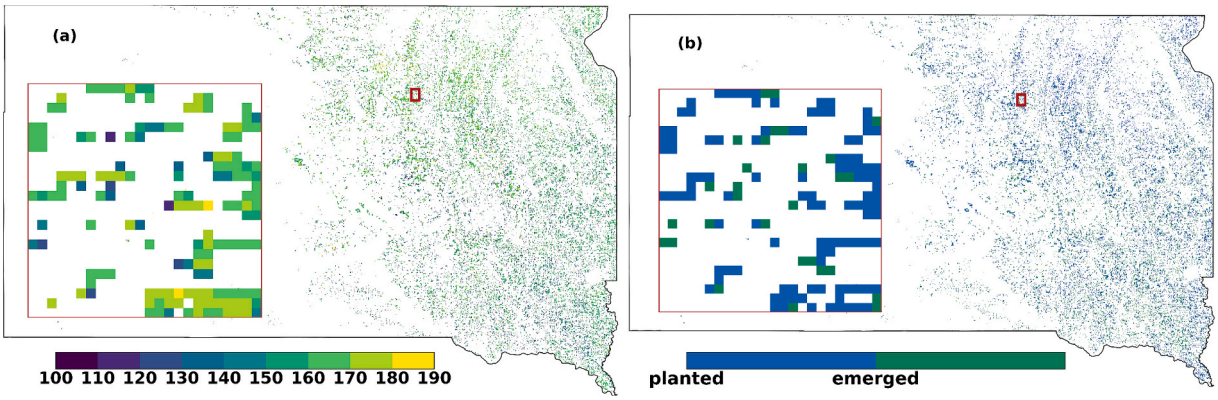

Fig. 13. Spatial patterns of soybean progress on DOY 156 in 2022 in South Dakota. (a) VIIRS-GLSP greenup onset, (b) GLSP crop progress for areas in planted and emerged stages.

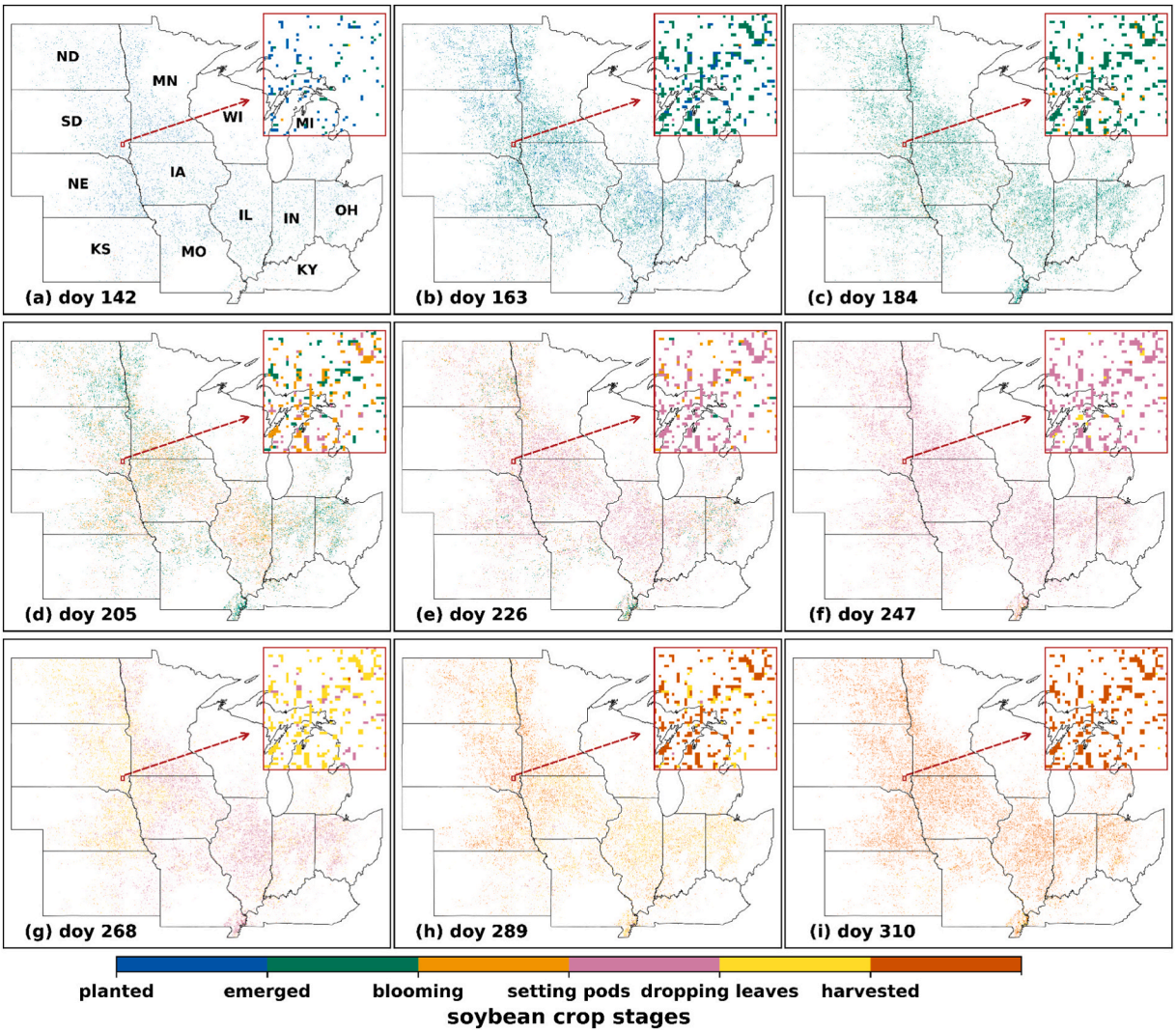

Fig. 14. Spatial patterns of GLSP crop progress for soybean growth during 2022 as estimated from VIIRS-GLSP phenometrics with every third week progress presented here starting from week 20 (DOY 142). The DOY of crop progress reported by NASS was used to create the weekly maps from GLSP crop progress. Illinois (IL), Indiana (IN), Iowa (IA), Kansas (KS), Kentucky (KY), Michigan (MI), Minnesota (MN), Missouri (MO), Nebraska (NE), North Dakota (ND), Ohio (OH), South Dakota (SD), Wisconsin (WI).

growth stages, allowing crops to mature earlier than usual. Precipitation patterns also played a key role in the inter-annual variation of crop progress, with excessive rainfall in the early growing season of 2019 (Gao et al. 2020; Shirzaei et al. 2021) leading to a notable shift in crop development stages. These variations were coincidently observed in the VIIRS-GLSP phenometrics although the phenological timing had a large

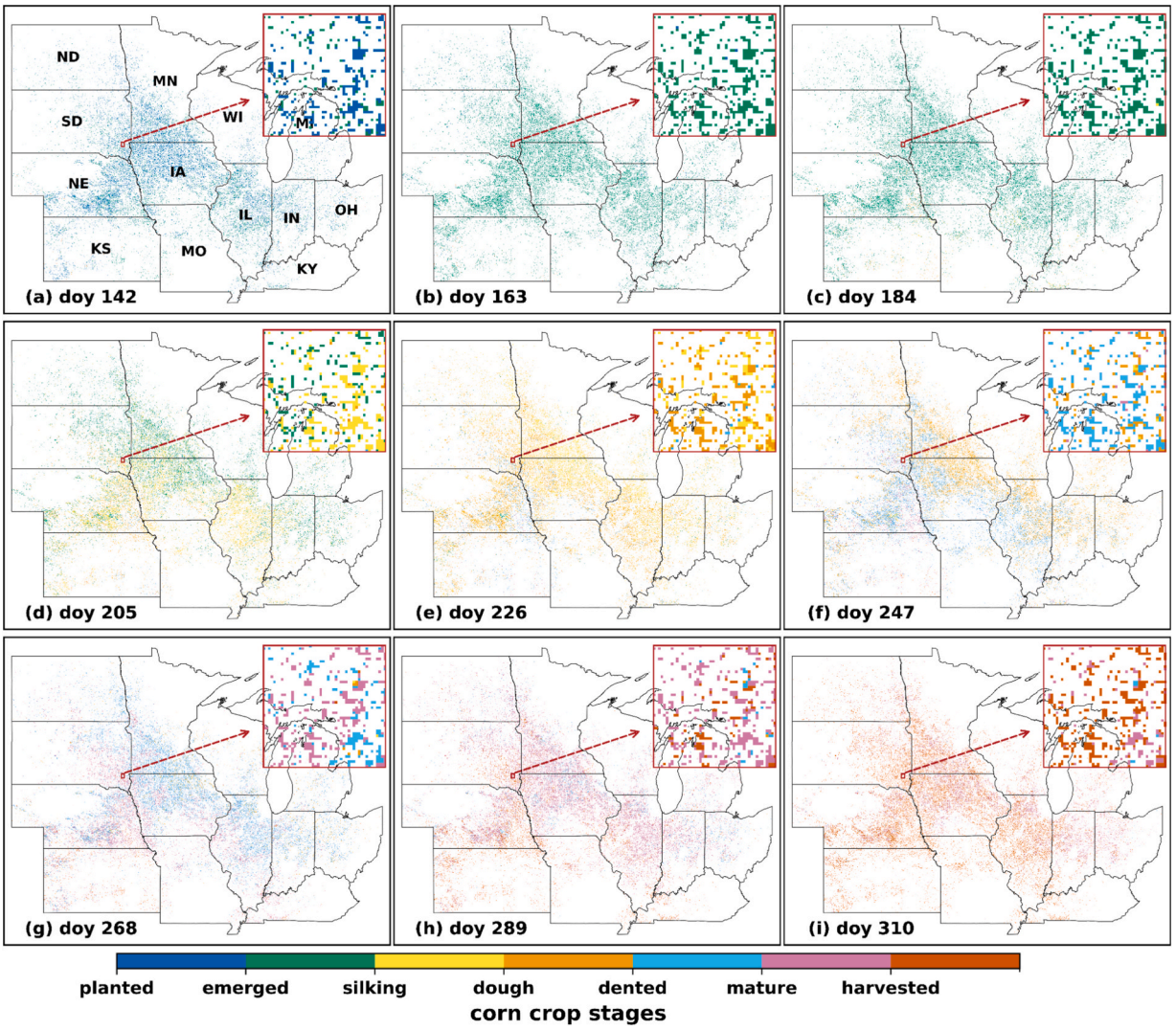

Fig. 15. Spatial patterns of GLSP crop progress for corn growth during 2022 as estimated from VIIRS-GLSP phenometrics with every third week progress presented here starting from week 20 (DOY 142). The DOY of crop progress reported by NASS was used to create the weekly maps from GLSP crop progress. Illinois (IL), Indiana (IN), Iowa (IA), Kansas (KS), Kentucky (KY), Michigan (MI), Minnesota (MN), Missouri (MO), Nebraska (NE), North Dakota (ND), Ohio (OH), South Dakota (SD), Wisconsin (WI).

shift relative to the NASS-CPR, which varied with individual phenological events and crop types. As expected, the VIIRS-GLSP greenup onset was consistently much later than NASS-CPR planted stage although they were significantly correlated with systematic biases (Bastidas et al. 2008). The VIIRS-GLSP greenup onset generally occurred later than NASS-CPR emerged dates in most cases. The late occurrence in greenup onset was likely attributed to the weak EVI2 signals at the early stages of crop emergence. Usually, greenup onset is detectable when crop coverage reaches 30 percent of the pixel (Zhang et al. 2017b) and two to four leaves have appeared (Gao et al. 2017). Further, the VIIRS-GLSP maturity onset was consistently earlier than NASS-CPR corn silking stage (Fig. 8c), which was supported by previous studies (Seo et al. 2019; Shen et al. 2022). Closely followed with NASS-CPR, the VIIRS-GLSP phenometrics showed large inter-annual shifts, which was attributed to various factors such as weather condition and crop management (Shen et al. 2022).

The crop progress derived from stage-one calibration of VIIRS-GLSP phenometrics, which was GLSP crop progress, was able to track NASS-CPR well, with some temporal differences. This was clearly illustrated for growth stages in soybean (Table 3) and corn (Table 4). Small RMSE values (< 5 days) in the GLSP crop progress were observed for the growth stages of soybean blooming, setting pods, and dropping leaves stages in Iowa, Kansas, Minnesota, Nebraska and South Dakota. Similarly, the GLSP crop progress estimated corn silking progress with a RMSE less than 6 days for all states except for Kansas. A similar pattern in the GLSP crop progress was observed for most stages of cotton rice and spring wheat in comparison with NASS-CPR (Tables S6-S8). On average, the GLSP crop progress showed a RMSE < 10 days for most crop stages across states. For all stages of cotton, the GLSP crop progress performed well in states (such as Alabama, Arizona, Arkansas, Georgia, Louisiana, Mississippi and North Carolina) with an average R^2 of 0.75 and an average RMSE of less than 7 days. For both rice and spring wheat, the GLSP crop progress showed strong performance across stages except for the harvest stage with a RMSE < 10 days in all states. The exception was rice in Louisiana where the performance of the GLSP crop progress was moderate. The bias in the estimates from the models was attributed to the limited ground truth data provided by NASS reporters across the CONUS, as well as the accuracy of VIIRS-GLSP phenometrics that were strongly impacted by the lack of high-quality observations (Zhang et al. 2018a).

The multi-year cross validation across environmentally diverse regions further demonstrates that the framework generalizes well across major CONUS production zones. The states analyzed span wide spatial gradients in planting timing, growing degree day accumulation,

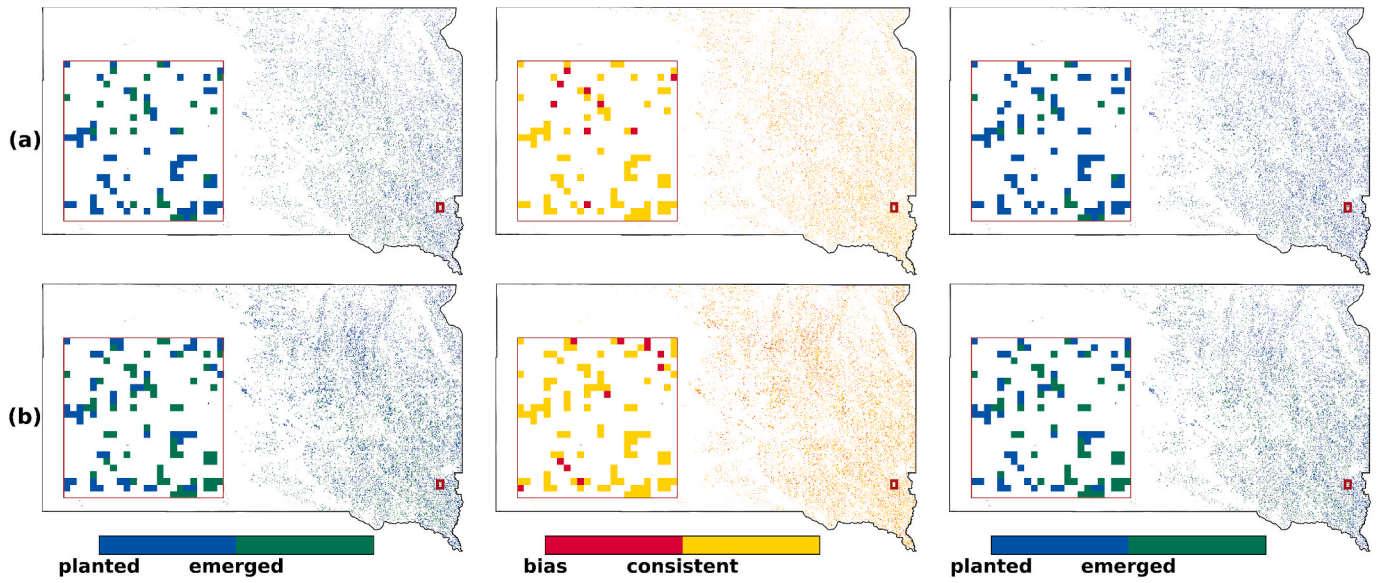

Fig. 16. Soybean crop progress maps including the GLSP crop progress map (left), the associated bias map (center), and the adjusted GLSP crop progress equivalent to NASS-CPR (right). The crop progress occurred on DOY 149 in the first row and on DOY 156 in the second row. The pixels flagged as bias were changed for the growth stages in the adjusted GLSP crop progress, while the pixels flagged as consistent remained the same in the GLSP crop progress and the adjusted GLSP crop progress.

precipitation regimes, and management practices. Despite this variability, the relationships between VIIRS-GLSP phenometrics and NASS-CPR stages remained stable, with mean cross validation RMSE values of <10 days across crops and states. This consistency indicates that the models effectively captured the dominant environmental controls on crop progress, supporting robust generalization from the state to regional scales.

Stage-specific accuracy varies systematically across the crop development stages. Early crop stages (planted and emerged) in the GLSP crop progress show relative higher RMSE, such as 11 days for soybean in Illinois, because both stages in NASS-CPR are linked to greenup onset. However, greenup onset is only detectable after sufficient canopy development and therefore lags field-reported dates as explained above (Gao et al. 2017; Zhang et al. 2017b). Mid-season reproductive growth stages (e.g., corn silking, soybean blooming, and heading stage for rice and spring wheat) are estimated using maturity onset with highest accuracy because canopy changes drive strong spectral responses. Relatively large errors are exhibited for later growth stages in the GLSP crop progress because they were linked to senescence onset (e.g., corn dough and dented), mid-senescence phase (e.g., corn mature and soybean dropping leaves) and dormancy onset (harvested), reflecting heterogeneity in senescence variability and harvest decisions within 500-m pixel. Additional sources of uncertainty include weak EVI2 sensitivity during early emergence and senescence, mixed pixels and heterogeneous within-pixel management at 500-m, and different subjectivity and quality of NASS-CPR across growth stages. These factors collectively amplify stage-specific discrepancies. Although the GLSP crop progress is an effective proxy for NASS-CPR (Figs. 11 and 12), future research activities are needed to reduce the uncertainties of model performance, particularly in early-season stages.

The GLSP crop progress from this study presented better or comparable accuracy relative to previous studies (Table 5). For corn in Illinois, our estimates for all stages were comparable to those produced from the hybrid phenology matching model (Diao et al. 2021) and the refined shape matching model (Sakamoto 2018). Specifically, the GLSP crop progress showed very good performance for critical silking stage with a

Table 5
Comparison of GLPS crop progress with previous studies using root means square error (RMSE) in days.

corn in Illinois							
	planted	emerged	silking	dough	dented	mature	harvested
This study	10.3	7.0	3.39	8.8	9.0	6.7	9.6
(Diao et al. 2021)	10.7	8.2	3.9	5.7	8.8	6.4	9.7
corn in Iowa							
This study	6.3	5.25	2.3	7.3	5.9	9.6	13.9
(Sakamoto 2018)	6.5	4.4	4.3	5.3	5.1	5.8	6.9
soybean in Illinois							
	planted	emerged	blooming	setting pods		dropping leaves	harvested
This study	11.0	11.1	7.6	12.9		8.7	7.0
(Diao et al. 2021)	5.4	4.3	7.1	5.6		3.8	6.5
(Diao 2020)		6.0	4.9	10.9		5.5	5.3
(Sakamoto 2018)	7.1	5.6	5.9	5.2		4.9	8.8
rice in Arkansas							
	planted		Emerged		headed		harvested
This study	5.3		6.0		3.9		5.6
(Sakamoto 2018)	6.4		5.5		5.9		5.8
spring wheat in North Dakota							
	planted		Emerged		headed		harvested
This study	5.2		3.9		1.8		10.5
(Sakamoto 2018)	8.7		7.2		7.3		5.5

RMSE of 3.4 days in Illinois and 2.3 days in Iowa, which were superior to the estimates produced by Diao et al. (2021) and Sakamoto (2018) respectively. Similarly, results from three reference studies (Diao 2020; Diao et al. 2021; Sakamoto 2018) support our findings for soybean progress estimation in Illinois. Although the RMSE scores were higher in Illinois, the model's accuracy for soybean growth stages across states was reasonable (Table 3). Similar patterns were observed for other crops. For cotton in Texas, cross-validation scores of our calibration models were consistent with those reported by Sakamoto (2018) although accuracy decreased for the testing year 2022. For rice and spring wheat in Arkansas and North Dakota, respectively, our estimates were superior to those of Sakamoto (2018) except spring wheat harvested stage.

The GLSP crop progress was further improved by applying a systematic stage-two adjustments using weekly NASS-CPR data for each growth stage. By comparing with weekly NASS-CPR percentages, bias adjustment was applied for the given weekly GLSP crop progress on each pixel through a stage-wise adjustment process. Although this adjustment redistributes some pixels between stages to achieve exact state-level agreement with NASS-CPR, it preserves the ordinal structure of calibrated phenology and the logical sequence of crop development, resulting in phenologically coherent spatial patterns. Because the adjustment relies on state-aggregated NASS-CPR percentages that could potentially mask sub-regional variability, the adjusted maps should be interpreted as NASS-consistent representations of broad regional patterns rather than field-level ground truth. Nevertheless, the weekly adjusted maps provide valuable insight into spatial heterogeneity in crop progress at sub-state scales, information not available directly from NASS-CPR.

The crop-progress estimates derived in this study are influenced by uncertainties originating from multiple components of the workflow. First, although the CDL provides high classification accuracies from 85% to 95% for major crops (Boryan et al. 2011), the 500-m pixels with a pure crop type aggregated from CDL could contain mixed vegetation types, particularly in regions with heterogeneous crop mosaics, which may bias the estimates of crop growth stages in 500-m pixels. Second, uncertainties inherent in the VIIRS-GLSP phenometrics arising especially from lack of high-quality temporal observations and the sensitivity of EVI2 at early emergence and late senescence can shift transition dates by several days (Zhang et al. 2024). Third, the stage-one calibration introduces additional uncertainty through subjective NASS-CPR data with limited field samples as well as the imperfect biophysical alignment between satellite-detected phenological events and NASS reported crop growth stages. This implies that finer pixel-level interpretations should be made with caution, while stage-one GLSP crop progress reliably depicts broad spatial patterns, seasonal progression, interannual anomalies and temporal trend assessment. Fourth, the stage-two cumulative-percentage adjustment ensures consistency with NASS-CPR at the state level, but it could redistribute pixels between stages, particularly when the cumulative curves between GLSP crop progress and NASS-CPR show considerable inconsistency. Although this adjustment preserves the relative ranking of pixels, it may locally alter fine-scale spatial gradients, indicating an inherent trade-off between maintaining spatial fidelity and enforcing agreement with official NASS-CPR statistics. Because of the complexity of error sources, quantitative analyses of error propagation remian very challenging, which needs future investigations.

Despite these uncertainties, the overall results remained robust. First, multi-year cross-validation (2013–2021) revealed model stability across contrasting agro-climatic conditions with mean RMSE values $<$10 days for all crops across states. Second, the stage-one calibration models consistently produce strong relationships between VIIRS-GLSP phenometrics and NASS-CPR (mean R^2 $>$0.7 across states and crop growth stages), despite inherent uncertainties of CDL, VIIRS-GLSP phenometrics, and state level aggregation of ground-based NASS crop progress. Third, the stage-two cumulative-percentage adjustment preserves the phenological order of pixels; thus, even when absolute timing is shifted, spatial gradients and phenological transitions remain biophysically meaningful. In addition, both stage-one and stage-two crop progress offer complementary value when interpreted together with former preserving natural spatial gradients and later enforcing consistency with NASS official statistics. Together, these findings confirm that although uncertainties may influence fine-scale variability, these do not compromise the operational utility of the approach.

Overall, the proposed VIIRS-GLSP calibration framework provides an operationally scalable approach for tracking crop progress and producing NASS-equivalent spatially explicit maps across the CONUS. The framework thus enabled retrospective reconstruction and prospective monitoring of crop progress, supporting agricultural decision-making, crop condition assessment, and long-term crop phenological analysis.

6. Conclusion

This study demonstrates the potential of VIIRS-GLSP phenometrics to enhance agricultural monitoring of crop progress by bridging the gap with ground-based agricultural observations. It proposed an approach for advancing crop monitoring by proving the ability of VIIRS-GLSP phenometrics to track crop progress equivalent to NASS-CPR for corn, soybean, cotton, rice, and spring wheat growth stages in diverse growing regions within the CONUS. The approach developed correlation models to bridge the VIIRS-GLSP phenometrics to the NASS-CPR data based on long-term observations comprised both normal and abnormal years, which improved generalizability and robustness and provided crop progress spatially at pixel levels. It was further adjusted using NASS-CPR observations at a given crop stage and week to improve the spatial pattern of the GLSP crop progress. The estimation of crop progress at 500-m pixels and weekly temporal resolution offers significant advantages for sustainable agriculture, enabling timely interventions and resource allocation. By addressing the identified limitations and incorporating additional data sources, future research can further enhance the reliability and applicability of remote sensing-derived phenometrics for agricultural decision-making. In summary, the proposed framework provides a robust and scalable method for generating spatially explicit and temporally consistent crop progress estimates using VIIRS-GLSP, bridging the gap between satellite phenology and field-based crop monitoring. Hence, the proposed approach is anticipated to be routinely implemented for operational monitoring of crop progress across CONUS.

CRediT authorship contribution statement

Naeem Abbas Malik: Writing – review & editing, Writing – original draft, Visualization, Validation, Methodology, Formal analysis, Data curation, Conceptualization. **Xiaoyang Zhang:** Writing – review & editing, Visualization, Validation, Supervision, Resources, Methodology, Investigation, Funding acquisition, Conceptualization. **Yu Shen:** Writing – review & editing, Writing – original draft, Visualization, Methodology. **Zhengwei Yang:** Writing – review & editing, Visualization, Methodology, Conceptualization. **Yongchang Ye:** Writing – review & editing, Visualization, Methodology. **Yuxia Liu:** Writing – review & editing, Visualization, Methodology.

Declaration of competing interest

The authors declare that they have no known competing financial interests or personal relationships that could have appeared to influence the work reported in this paper.

Acknowledgements

This work was supported by the United States Department of Agriculture (USDA) under grant number 2023-67021-40549 and the National Aeronautics and Space Administration (NASA) under grant number 80NSSC21K1962. Additional support was provided by the

Higher Education Commission of Pakistan and Pir Mehr Ali Shah Arid Agriculture University Rawalpindi Pakistan. We also gratefully acknowledge The Research Cyberinfrastructure (RCi) team at South Dakota State University for their support for high-performance computing.

Appendix A. Supplementary data

Supplementary data to this article can be found online at https://doi.org/10.1016/j.isprsjprs.2026.02.032.

References

Bastidas, A.M., Setryono, T.D., Dobermann, A., Cassman, K.G., Elmore, R.W., Graef, G.L., Specht, J.E., 2008. Soybean sowing date: the vegetative, reproductive, and agronomic impacts. Crop Sci. 48, 727–740.

Boryan, C., Yang, Z.W., Mueller, R., Craig, M., 2011. Monitoring US agriculture: the US Department of Agriculture, National Agricultural Statistics Service, Cropland Data Layer Program. Geocarto Int. 26, 341–358.

Brown, M.E., de Beurs, K.M., Marshall, M., 2012. Global phenological response to climate change in crop areas using satellite remote sensing of vegetation, humidity and temperature over 26 years. Remote Sens. Environ. 126, 174–183.

Chen, Y., Zhang, Z., Tao, F.L., 2018. Improving regional winter wheat yield estimation through assimilation of phenology and leaf area index from remote sensing data. Eur. J. Agron. 101, 163–173.

Diao, C.Y., 2020. Remote sensing phenological monitoring framework to characterize corn and soybean physiological growing stages. Remote Sens. Environ. 248.

Diao, C.Y., Yang, Z.J., Gao, F., Zhang, X.Y., Yang, Z.W., 2021. Hybrid phenology matching model for robust crop phenological retrieval. ISPRS J. Photogramm. Remote Sens. 181, 308–326.

Franch, B., Vermote, E.F., Becker-Reshef, I., Claverie, M., Huang, J., Zhang, J., Justice, C., Sobrino, J.A., 2015. Improving the timeliness of winter wheat production forecast in the United States of America, Ukraine and China using MODIS data and NCAR growing Degree Day information. Remote Sens. Environ. 161, 131–148.

Gao, F., Anderson, M., Daughtry, C., Karnieli, A., Hively, D., Kustas, W., 2020. A within-season approach for detecting early growth stages in corn and soybean using high temporal and spatial resolution imagery. Remote Sens. Environ. 242.

Gao, F., Anderson, M.C., Zhang, X.Y., Yang, Z.W., Alfieri, J.G., Kustas, W.P., Mueller, R., Johnson, D.M., Prueger, J.H., 2017. Toward mapping crop progress at field scales through fusion of Landsat and MODIS imagery. Remote Sens. Environ. 188, 9–25.

Gao, F., & Zhang, X.Y. (2021). Mapping Crop Phenology in Near Real-Time Using Satellite Remote Sensing: Challenges and Opportunities. *Journal of Remote Sensing, 2021*.

Gim, H.J., Ho, C.H., Jeong, S., Kim, J., Feng, S., Hayes, M.J., 2020. Improved mapping and change detection of the start of the crop growing season in the US Corn Belt from long-term AVHRR NDVI. Agric. For. Meteorol. 294.

Kosczor, E., Forkel, M., Hernández, J., Kinalczyk, D., Pirotti, F., Kutchartt, E., 2022. Assessing land surface phenology in Araucaria-Nothofagus forests in Chile with Landsat 8/Sentinel-2 time series. Int. J. Appl. Earth Obs. Geoinf. 112.

Li, S.H., Xiao, J.T., Ni, P., Zhang, J., Wang, H.S., Wang, J.X., 2014. Monitoring paddy rice phenology using time series MODIS data over Jiangxi Province, China. Int. J. Agric. Biol. Eng. 7, 28–36.

Liu, L.L., Zhang, X.Y., Yu, Y.Y., Gao, F., Yang, Z.W., 2018. Real-Time monitoring of Crop Phenology in the Midwestern United States using VIIRS Observations. Remote Sens. (Basel) 10.

Luo, Y.C., Zhang, Z., Chen, Y., Li, Z.Y., Tao, F.L., 2020. ChinaCropPhen1km: a high-resolution crop phenological dataset for three staple crops in China during 2000-2015 based on leaf area index (LAI) products. Earth Syst. Sci. Data 12, 197–214.

NASS (2018). National Crop Progress - Terms and Definitions.

Onojeghuo, A.O., Blackburn, G.A., Wang, Q.M., Atkinson, P.M., Kindred, D., Miao, Y.X., 2018. Rice crop phenology mapping at high spatial and temporal resolution using downscaled MODIS time-series. Giscience & Remote Sensing 55, 659–677.

Sakamoto, T., 2018. Refined shape model fitting methods for detecting various types of phenological information on major US crops. ISPRS J. Photogramm. Remote Sens. 138, 176–192.

Sakamoto, T., Wardlow, B.D., Gitelson, A.A., 2011. Detecting spatiotemporal changes of corn developmental stages in the US Corn Belt using MODIS WDRVI Data. IEEE Trans. Geosci. Remote Sens. 49, 1926–1936.

Sakamoto, T., Wardlow, B.D., Gitelson, A.A., Verma, S.B., Suyker, A.E., Arkebauer, T.J., 2010. A Two-step Filtering approach for detecting maize and soybean phenology with time-series MODIS data. Remote Sens. Environ. 114, 2146–2159.

Sakamoto, T., Yokozawa, M., Toritani, H., Shibayama, M., Ishitsuka, N., Ohno, H., 2005. A crop phenology detection method using time-series MODIS data. Remote Sens. Environ. 96, 366–374.

Sehgal, V.K., Jain, S., Aggarwal, P.K., Jha, S., 2011. Deriving crop phenology metrics and their trends using times series NOAA-AVHRR NDVI Data. J. Indian Soc. Remote Sens. 39, 373–381.

Seo, B., Lee, J., Lee, K.D., Hong, S., Kang, S., 2019. Improving remotely-sensed crop monitoring by NDVI-based crop phenology estimators for corn and soybeans in Iowa and Illinois, USA. Field Crop Res 238, 113–128.

Shen, Y., Zhang, X.Y., Yang, Z.W., 2022. Mapping corn and soybean phenometrics at field scales over the United States Corn Belt by fusing time series of Landsat 8 and Sentinel-2 data with VIIRS data. ISPRS J. Photogramm. Remote Sens. 186, 55–69.

Shen, Y., Zhang, X.Y., Yang, Z.W., Ye, Y.C., Wang, J.M., Gao, S., Liu, Y.X., Wang, W.L., Tran, K.H., Ju, J.C., 2023. Developing an operational algorithm for near-real-time monitoring of crop progress at field scales by fusing harmonized Landsat and Sentinel-2 time series with geostationary satellite observations. Remote Sens. Environ. 296.

Shirzaei, M., Khoshmanesh, M., Ojha, C., Werth, S., Kerner, H., Carlson, G., Sherpa, S.F., Zhai, G., Lee, J.C., 2021. Persistent impact of spring floods on crop loss in U.S. Midwest. Weather Clim. Extremes 34.

Sisheber, B., Marshall, M., Ayalew, D., Nelson, A., 2022. Tracking crop phenology in a highly dynamic landscape with knowledge-based Landsat-MODIS data fusion. Int. J. Appl. Earth Obs. Geoinf. 106.

Thapa, S., Millan, V.E.G., Eklundh, L., 2021. Assessing Forest Phenology: a Multi-Scale Comparison of Near-Surface (UAV, Spectral Reflectance Sensor, PhenoCam) and Satellite (MODIS, Sentinel-2) Remote Sensing. Remote Sens. (Basel) 13.

Tran, K.H., Zhang, X.Y., Ye, Y.C., Shen, Y., Gao, S., Liu, Y.X., Richardson, A., 2023. HP-LSP: a reference of land surface phenology from fused Harmonized Landsat and Sentinel-2 with PhenoCam data. Sci. Data 10.

USDA (2015). Crop production 2014 summary.

USDA (2018). Crop production 2017 summary.

USDA (2020). Crop production 2019 summary.

Walthall, C.L.A., Chirstopher, J., Raumgard., L.H., Takle, E., & Wright-Morton, L. (2013). Climate Change and Agriculture in the United States: Effects and Adaptation.

Wu, W., Sun, Y., Xiao, K., Xin, Q.C., 2021. Development of a global annual land surface phenology dataset for 1982-2018 from the AVHRR data by implementing multiple phenology retrieving methods. Int. J. Appl. Earth Obs. Geoinf. 103.

Yang, Y.J., Ren, W., Tao, B., Ji, L., Liang, L., Ruane, A.C., Fisher, J.B., Liu, J.G., Sama, M., Li, Z., Tian, Q.J., 2020. Characterizing spatiotemporal patterns of crop phenology across North America during 2000-2016 using satellite imagery and agricultural survey data. ISPRS J. Photogramm. Remote Sens. 170, 156–173.

Zhang, X., Henebry, G.M., Friedl, M.A., Schaaf, C., Ye, Y., Tran, K., & Liu, L. (2024). Algorithm Technical Basis Document, VIIRS Land Surface Phenology Product.

Zhang, X.Y., 2015. Reconstruction of a complete global time series of daily vegetation index trajectory from long-term AVHRR data. Remote Sens. Environ. 156, 457–472.

Zhang, X.Y., Jayavelu, S., Liu, L.L., Friedl, M.A., Henebry, G.M., Liu, Y., Schaaf, C.B., Richardson, A.D., Gray, J., 2018a. Evaluation of land surface phenology from VIIRS data using time series of PhenoCam imagery. Agric. For. Meteorol. 256, 137–149.

Zhang, X.Y., Liu, L.L., Liu, Y., Jayavelu, S., Wang, J.M., Moon, M., Henebry, G.M., Friedl, M.A., Schaaf, C.B., 2018b. Generation and evaluation of the VIIRS land surface phenology product. Remote Sens. Environ. 216, 212–229.

Zhang, X.Y., Liu, L.L., Yan, D., 2017a. Comparisons of global land surface seasonality and phenology derived from AVHRR, MODIS, and VIIRS data. J. Geophys. Res.-Biogeosci. 122, 1506–1525.

Zhang, X.Y., Wang, J.M., Gao, F., Liu, Y., Schaaf, C., Friedl, M., Yu, Y.Y., Jayavelu, S., Gray, J., Liu, L.L., Yan, D., Henebry, G.M., 2017b. Exploration of scaling effects on coarse resolution land surface phenology. Remote Sens. Environ. 190, 318–330.

Zhang, X.Y., Wang, J.M., Henebry, G.M., Gao, F., 2020. Development and evaluation of a new algorithm for detecting 30 m land surface phenology from VIIRS and HLS time series. ISPRS J. Photogramm. Remote Sens. 161, 37–51.